Berridge 2002). Altered function of the mPFC has been implicated in multiple processes and behavioural disorders, including schizophrenia (Weinberger 1995), drug abuse (Wise, Murray & Gerfen 1996), depression (Merriam *et al.* 1999) and attention deficit hyperactivity disorder (Puumala & Sirvio 1998) as well as normal cognitive processes, including working memory function (Williams & Goldman-Rakic 1995; Jentsch *et al.* 1997a,b) and decision making (Damasio 1995). The mPFC has received considerable attention with respect to its involvement in reward-related mechanisms (Tzschentke & Schmidt 2000). Noradrenaline (NA) release in the mPFC has been recently considered as crucial in mediating rewarding effects of opioids (Ventura, Alcaro & Puglisi-Allegra 2005). Despite the importance of prefrontal cortical dopamine, as well as NA, in modulating reward, cognition and behaviour, little is known about the involvement of dopamine that regulate the rewarding effects of opioids in the mPFC.

The anterior cingulate cortex (ACG), a major subregion of the prefrontal cortex, is involved in evaluative processes. The ACG might also serve to encode whether or not an action is worth performing in view of the expected benefit and the cost of performing the action (Rushworth *et al.* 2004). For instance, after excitotoxic ACG lesions, rats no longer selected the high cost–high reward option in a cost–benefit T-maze task if they had to choose between climbing a barrier to obtain a large reward in one arm or running for a low reward into the other arm with no barrier present (Walton *et al.* 2003). Recent studies have indicated that mesocortical dopamine fibres projecting to the ACG (Berger, Gaspar & Verney 1991) may be responsible for effort-based decision-making (Schweimer, Saft & Hauber 2005). In addition, the ACG contributes to the generation of emotional states and to the executive control of behavioural selection (Peoples 2002).

In the present study, we therefore investigated the role of dopaminergic neurons projecting from the VTA possibly to the ACG in μ-opioid reward.

MATERIALS AND METHODS

The present study was conducted in accordance with the Guiding Principles for the Care and Use of Laboratory Animals (Hoshi University) as adopted by the Committee on Animal Research of Hoshi University, which is accredited by the Ministry of Education, Culture, Sports, Science, and Technology of Japan. Every effort was made to minimize the number and suffering of animals used in the following experiments.

Animals

In the present study, we used male Sprague Dawley rats (200–250 g) (Tokyo Laboratory Animals Science, Tokyo, Japan). The animals were housed in a room maintained at 23 ± 1°C with a 12-hour light/dark cycle (lights on 8 AM to 8 PM). Food and water were available *ad libitum*.

Drugs

The drugs used in the present study were morphine hydrochloride (Daiichi-Sankyo, Tokyo, Japan), 6-hydroxydopamine hydrochloride (6-OHDA), desipramine hydrochloride, (D-Ala^2, *N*-MePhe^4, Gly-ol^5) enkephalin (DAMGO) (Sigma-Aldrich, St. Louis, MO), R(+)-7-chloro-8-hydroxy-3-methyl-1-phenyl-2,3,4,5-tetrahydro-1H-3-benzazepine hydrochloride (SCH23390; Sigma Chemical Co., MO, USA), fluorogold (FG; fluorochrome, Englewood, CO, USA), and cholera toxin B Alexa Fluor 555 conjugate (CTb; Invitrogen, Grand Island, NY, USA).

Experiments I

In retrograde tracing study, the rats were deeply anesthetized with sodium pentobarbital (50 mg/kg, i.p.) and placed in a stereotaxic apparatus. The skull was exposed, and a hole was drilled through the skull over the ACG (from bregma: anterior +1.7 mm; lateral +0.4 mm; and ventral −2.8 mm) or N.Acc (from bregma; anterior +1.5 mm; lateral +2.7 mm; and ventral −7.3 mm; angle 10°) according to the atlas of Paxinos and Watson (Paxinos & Watson 1998). Except pressure-injected (200 nl) into the ACG in the FG (fluorochrome, 4% solution in saline) injection, micropipettes of about 20–23 μm in diameter were filled with FG solution, and the tracer was injected into the N.Acc for 25 minutes by iontophoresis with a positive-pulsed current (5 μA, seven seconds on/off intervals). The micropipette was left in place for five minutes following the completion of injection to avoid leakage of the tracer along the pipette track, and then the pipette was withdrawn from the brain. In the CTb (Invitrogen) injection, the injection cannula was filled with CTb (1 mg/ml) solution, and CTb was pressure-injected (1 μl) into the ACG. The CTb, as well as FG, was used as retrograde tracer (Kishi *et al.* 2006; Almarestani *et al.* 2007; Steen *et al.* 2007). After the injection, the injection cannula was left in place for five minutes. Five days after the injections, the animals were perfused as described later. The distributions of FG or CTb retrogradely labelled neurons and FG or CTb injection sites were detected using a microscope (Olympus BX-60; Olympus, Tokyo, Japan). In perfusion and tissue processing, the rats were deeply anesthetized with 3% isoflurane and perfusion-fixed with 4% paraformaldehyde, pH 7.4. The brains were then quickly removed after perfusion, and thick coronal sections of the ACG, N.Acc or VTA were initially dissected using brain blocker (Neuroscience, Tokyo, Japan). The brain coronal sections were post-fixed in 4% paraformaldehyde for three hours. After the brains

were permeated with 20% sucrose for one day and 30% sucrose for two days, they were frozen in embedding compound (Sakura Finetechnical, Tokyo, Japan) on isopentane using liquid nitrogen and stored at −30°C until use. Frozen 8 μm-thick coronal sections were cut with a cryostat (CM1510; Leica, Heidelberg, Germany) and thaw-mounted on poly-L-lysine-coated glass slides. In immunohistochemical approach, the brain sections were blocked in serum in 0.01 mol/l phosphate buffer saline (PBS) for one hour at 23 ± 1°C. Each primary antibody was diluted in 0.01 mol/l PBS containing 10% normal goat serum (NGS) [1:25, 1:40 or 1:60 tyrosine hydroxylase (TH; mouse monoclonal, MAB358, Chemicon, Temecula, CA, USA)] and incubated for two days at 4°C. The samples were then rinsed and incubated with the appropriate secondary antibody conjugated with Alexa 488 and Alexa 546 for two hours at 23 ± 1°C. The slides were then coverslipped with PermaFluor Aqueous mounting medium (Immunon, Pittsburgh, PA, USA). Fluorescence of immunolabelling was detected using a light microscope (Olympus BX-60) and U-MWIG and U-MNIBA filter cubes (Olympus) for an Alexa 488 or Alexa 546. Digitized images of the ACG, N.Acc or VTA sections were captured at a resolution of 1316 × 1035 pixels with a camera (Polaroid PDMCII/OL; Olympus). The upper and lower threshold density ranges were adjusted to encompass and match the immunoreactivity (IR) to provide an image in which IR material appeared as white pixels and non-IR material appeared as black pixels.

Experiments II

In surgery and microinjection, after three days of habituation to the main animal colony, all of the rats were anesthetized with sodium pentobarbital (50 mg/kg, i.p.). The anesthetized animals were placed in a stereotaxic apparatus. The skull was exposed, and a small hole was made using a dental drill. A guide cannula (AG-9, AG-8 or AG-4; Eicom, Kyoto, Japan) or an electrode (NS303/12; Bioresearch Center, Nagoya, Japan) was implanted into the VTA (from bregma: anterior, −5.3 mm; lateral, −0.9 mm; ventral, −7.7 mm or anterior, −6.8 mm; lateral, ±0.9 mm; ventral, −7.8 mm; angle 10°), ACG [from bregma: anterior, +1.7 mm; lateral, −0.4 mm; ventral, −1.1 mm (*in vivo* microdialysis) or −2.3 mm (microinjection)] or N.Acc (from bregma: anterior, +4.0 mm; lateral, −0.8 mm; ventral, −6.8 mm; angle 16°) according to the atlas of Paxinos & Watson (1998). The guide cannula or the electrode was fixed to the skull with cranioplastic cement. In the microinjection method, we used an injection cannula (AMI-9.5; Eicom) that extended beyond the guide cannula by 0.5 mm. A stainless steel injection cannula was inserted into the guide cannula for each animal. The injection cannula was connected through polyethylene tubing to a 10 μl Hamilton syringe that was preloaded with DAMGO (1 nmol/0.3 μl) or saline. DAMGO or saline was delivered by a motorized syringe pump in a volume of 0.3 μl over 60 seconds. In *in vivo* microdialysis study, three to five days after the surgery, microdialysis probes (AI-4-2 or AI-8-2; 2 mm membrane length; Eicom) were slowly inserted into the ACG or N.Acc through guide cannulas under anaesthesia with diethyl ether, and the rats were settled in the experimental cages (30 cm wide × 30 cm deep × 30 cm high). The probes were perfused continuously at a flow rate of 2 μl/minute with artificial cerebrospinal fluid (aCSF) containing 0.9 mM $MgCl_2$, 147.0 mM NaCl, 4.0 mM KCl and 1.2 mM $CaCl_2$. The outflow fractions were taken every 20 minutes. After three baseline fractions were collected in the rat ACG or N.Acc, DAMGO or saline was administered into the rat VTA using a 10 μl Hamilton syringe and a motorized syringe pump. For these experiments, dialysis samples were collected for 180 minutes after DAMGO or saline treatment. Dialysis fractions were then analyzed using HPLC (Eicom) with an electrochemical detection (ECD) (Eicom) system. Dopamine was separated by a column with a mobile phase containing sodium acetate (4.05 g/l), citric acid monohydrate (7.35 g/l), sodium 1-octane sulfonate (150 mg/l), EDTA (2Na; 10 mg/l) and 17% methanol. The mobile phase was delivered at a flow rate of 210 μl/minute. Dopamine was identified according to the retention time of a dopamine standard, and the peak area of basal dopamine was divided by the peak area of a dopamine standard to obtain the amount of basal dopamine. In electrical stimulation, three to five days after surgery, microdialysis probes were inserted and an *in vivo* microdialysis study was performed as described earlier. Electrical stimulation (stimulation intensity of 100 or 150 μA, stimulation frequency of 100 Hz, 0.5-second trains of 0.5-m second pulses, interval of two seconds) was applied to the VTA for 40 minutes after three baseline fractions were collected in the rat ACG. This stimulation was delivered by constant-current stimulators via a bipolar cable (Bioresearch Center) connected to the electrode.

Experiments III

Immunohistochemical study was conducted as described earlier. Each primary antibody was diluted in 0.01 mol/l PBS containing 10% NGS [1:25, 1:40 or 1:60 tyrosine hydroxylase (mouse monoclonal, MAB358)] or 20% NGS in 0.1% Triton X-100 [1 : 3500 MOR (rabbit polyclonal, RA10104, Neuromics, Bloomington, MN, USA)]. The microinjection of retrograde tracer was conducted as described earlier.

Experiments IV

Place conditioning was conducted as described previously (Suzuki, Masukawa & Misawa 1990). The biased

design was used for place conditioning. The apparatus was a shuttle box (30 cm wide × 60 cm long × 30 cm high) that was made of acrylic resin board and divided into two equal-sized compartments. One compartment was white with a textured floor, and the other was black with a smooth floor to create equally preferable compartments. The place conditioning schedule was composed of three phases (pre-conditioning test, conditioning, and post-conditioning test). The pre-conditioning test was performed as follows: the partition separating the two compartments was raised to 12 cm above the floor, a neutral platform was inserted along the seam separating the compartments and the animals that had not been treated with either drugs or saline were then placed on the platform. The time spent in each compartment during a 900-seconds session was then recorded automatically with an infrared beam sensor (KN-80; Natsume Seisakusyo, Tokyo, Japan). Conditioning sessions (three days for DAMGO (0.3, 1, 3, 9 nmol/0.3 μl) or morphine (8 or 23 mg/kg, i.p.), three days for saline) were conducted once daily for six days. Immediately after DAMGO injection or treatment with morphine, these animals were placed in the compartment opposite that in which they had spent the most time in the pre-conditioning test for one hour. On alternating days, these animals received saline and were placed in the other compartment for one hour. On the day after the final conditioning session, a post-conditioning test that was identical to the pre-conditioning test was performed. To destroy central dopaminergic neurons, 6-OHDA (8 μg/0.3 μl) was injected into the ACG of the rats four days before the start of conditioning with DAMGO or morphine. Additionally, desipramine (20 mg/kg, s.c.) was given to rats 30 minutes before the injection of 6-OHDA into the ACG to block the uptake of 6-OHDA into noradrenergic terminals (Alhaider 1991). To investigate the extinction of the morphine- or DAMGO-induced place preference, a post-conditioning test was performed with no conditioning and was conducted at 1 day, 9 days, 13 days or 20 days after the final conditioning test. Immunohistochemical study was conducted as described earlier. Primary antibody was diluted in 0.01 mol/l PBS containing 10% NGS [1:1000 TH (rabbit polyclonal, AB152, Chemicon)]. In high-pressure liquid chromatography (HPLC) study, the rats were killed four days after the microinjection of saline or 6-OHDA (8 μg/0.3 μl) in combination with s.c. injection of vehicle or desipramine. The brain was removed quickly, and the ACG was dissected on an ice-cold glass plate. The tissues were homogenized in 1000 μl of 0.2 M perchloric acid containing 100 mM EDTA(2Na) and 140 ng isoproterenol as an internal standard. The homogenates were then centrifuged at 20 000 ×g for 32 minutes at 4°C, and the supernatants were maintained at pH 3.0 using 1 M sodium acetate. The samples were analyzed by HPLC-ECD. The HPLC system was composed of a delivery system (EP-10; Eicom), an analytical column (Eicompac, SC-5ODS; Eicom) and a guard column (Eicom). Dopamine and its metabolites were separated by a column with a mobile phase containing sodium acetate (3.22 g/l), citric acid monohydrate (9.17 g/l), sodium 1-octane sulfonate (180 mg/l), EDTA(2Na) (10 mg/l) and 17% methanol. The mobile phase was delivered at a flow rate of 0.5 ml/minute. Dopamine and its metabolites were identified according to the retention times of these standards, and the peak heights of dopamine and its metabolites revised internal standard was divided by the peak heights of those standard revised internal standard to obtain those amount.

Experiments V

Place conditioning was performed as described earlier. In treatment with SCH23390, the rats were administered saline or SCH23390 (0.1 mg/kg, i.p.) 15 minutes before the treatment with morphine. In Western blotting, 24 hours or 10 days after the final conditioning in the conditioned place preference (CPP) procedure described earlier, the rats were sacrificed by decapitation. The ACG was quickly removed after decapitation and homogenized in ice-cold buffer. The homogenate was centrifuged at 20 000 ×g for 10 minutes and the supernatant was retained as the lysate fraction for Western blotting. An aliquot of tissue sample was diluted with an equal volume of 2× electrophoresis sample buffer (Protein Gel Loading Dye-2X, Amresco, Solon, OH, USA) containing 2% sodium dodecyl sulfate (SDS) and 10% glycerol with 0.2 M dithiothreitol. Proteins (7 μl/lane) were separated by size on 4–20% SDS-polyacrylamide gradient gel by using the buffer system of Laemmli (1970) and transferred to nitrocellulose membranes in Tris-glycine buffer containing 25 mM Tris and 192 mM glycine. For immunoblot detection, the membranes were blocked in Tris-buffered saline (TBS) containing 1% non-fat dried milk (Bio-Rad Laboratories, Hercules, CA, USA) containing 0.1% Tween 20 (Research Biochemicals, Natick, MA, USA) for one hour at room temperature with agitation. The membrane was incubated with primary antibody diluted in 1:1000 phosphorylated dopamine and cyclic AMP-regulated phosphoprotein with molecular weight 32 kDa (p-DARPP32; rabbit, #2304, Cell Signaling Technology, Danvers, CA, USA) and 1:1000 phosphorylated cAMP response element binding protein (p-CREB; rabbit, #9191, Cell Signaling Technology), 1:200 000 glyceraldehyde-3-phosphate dehydrogenase (GAPDH; mouse monoclonal, MAB374, Chemicon International, Temecula, CA, USA) containing 1% non-fat dried milk containing 0.1% Tween 20 overnight at 4°C. The membrane was washed in TBS containing 0.05% Tween 20

(TTBS), and then incubated for two hours at room temperature with horseradish peroxidase-conjugated goat anti-rabbit IgG (Southern Biotechnology Associates, Birmingham, AL, USA) diluted 1:10 000 in TBS containing 1% non-fat dried milk with 0.1% Tween 20. After this incubation, the membranes were washed in TTBS. The antigen-antibody peroxidase complex was finally detected by enhanced chemiluminescence (Pierce, Rockford, IL, USA) according to the manufacturer's instructions and visualized by exposure to Amersham Hyperfilm (Amersham Life Sciences, Arlington Heights, IL, USA).

Histology

The locations of the infusion cannula and drug diffusion were assessed at the completion of the experiments. The rats were deeply anesthetized with sodium pentobarbital at the end of the experiment and given microinjections of ink for the anatomical localization of cannula sites (0.3 μl). The brain was then removed by decapitation and cut into coronal sections. Cannula locations were mapped onto a stereotaxic atlas (Paxinos & Watson 1998) and confirmed to be in the VTA, ACG or N.Acc.

Statistical data analysis

Dates are expressed as the mean with SEM. One- and two-way analyses of variance (ANOVAs) with independent and repeated measures as well as planned comparisons or Student's *t*-tests, were used as appropriate for the experimental design. Multiple comparisons were performed using Dunnet or Bonferroni *post hoc* test where appropriate. The potency ratio for the saline-treated rats and the 6-OHDA-treated rats were calculated by the parallel line assay (Tallarida, Porreca & Cowan 1989).

RESULTS

Experiments I

Dopamine neurons projecting from the VTA to the ACG

To determine whether the VTA is linked to the ACG, we investigated whether there were any neuronal projections from the VTA to the ACG using FG as a retrograde tracer. Schematic illustrations of the injection site in the ACG (CG1, CG2) or N.Acc are shown with the symbols (Fig. 1a, b). Pressure application of FG into the region of the unilateral ACG produced a well-restricted injection site (Fig. 1c). FG-labelled cell bodies (Fig. 1d) or TH-labelled cells (Fig. 1e) were apparently detected in the VTA after the microinjection of FG into the ACG. A population of retrogradely labelled neurons in the VTA also showed TH-IR (Fig. 1f).

Distribution of cell bodies of neurons projecting from the VTA to the ACG or N.Acc

To investigate whether neurons that projected from the VTA to the ACG or N.Acc were independent, the retrograde tracers CTb and FG were microinjected into the unilateral ACG and N.Acc, respectively (Fig. 1g, h). FG- or CTb-containing cells were detected in the VTA after the microinjection of FG or CTb. FG-labelled neurons and CTb-labelled neurons did not overlap in the VTA (Fig. 1i).

Experiments II

Dialysate dopamine level in the ACG by electrical stimulation in the VTA

To further verify the dopaminergic neurons projecting from the VTA to the ACG, we examined the effect of the electrical stimulation of VTA cells on dopamine release in the ACG. In an *in vivo* microdialysis study, the basal levels of dopamine and the major dopamine metabolites, 3,4-dihydroxyphenylacetic acid (DOPAC) and homovanillic acid (HVA), in the ACG were lower than that of dopamine in the N.Acc ($n = 5$) ($^{*}P < 0.05$, $^{**}P < 0.01$ versus dopamine, DOPAC or HVA in the N.Acc) (Table 1). The dopamine levels in the ACG were increased by the electrical stimulation of VTA cells ($n = 5$) (Fig. 2a). The electrical stimulation of VTA cells also increased the levels of DOPAC and HVA ($n = 5$) (Fig. 2b, c). Statistical analysis was performed with one-way ANOVA followed by Dunnet test (dopamine, $F_{(7,28)} = 3.710$, $P < 0.01$; DOPAC, $F_{(7,28)} = 7.426$, $P < 0.001$; HVA, $F_{(7,28)} = 12.04$, $P < 0.001$) ($^{*}P < 0.05$, $^{**}P < 0.01$, $^{***}P < 0.001$ versus 0 minute).

Dialysate dopamine level in the ACG under the microinjection of a μ-opioid receptor agonist into the VTA

We next investigated the change in the dialysate dopamine level in the ACG under the intra-VTA administration of a μ-opioid receptor agonist. Schematic illustrations of dialysis probe placements in the ACG or N.Acc are shown in Fig. 3a, b. The dopamine level was markedly increased by the injection of DAMGO compared with saline treatment in the ACG ($n = 5$) (Fig. 3c). The injection of DAMGO into the VTA also produced a significant increase in DOPAC and HVA in the ACG ($n = 5$) (Fig. 3d, e). Statistical analysis was performed with two-way ANOVA followed by Bonferroni test [dopamine: interaction between treatment and time: $F_{(11,88)} = 1.972$, $P < 0.05$; effect of treatment, $F_{(1,88)} = 5.841$, $P < 0.05$; effect of time, $F_{(11,88)} = 3.250$ $P < 0.001$; DOPAC: interaction between treatment and time: $F_{(11,88)} = 7.278$, $P < 0.001$; effect of treatment, $F_{(1,88)} = 22.77$, $P < 0.01$; effect of time, $F_{(11,88)} = 12.60$, $P < 0.001$; HVA: interaction between treatment and time: $F_{(11,88)} = 3.823$, $P < 0.001$; effect

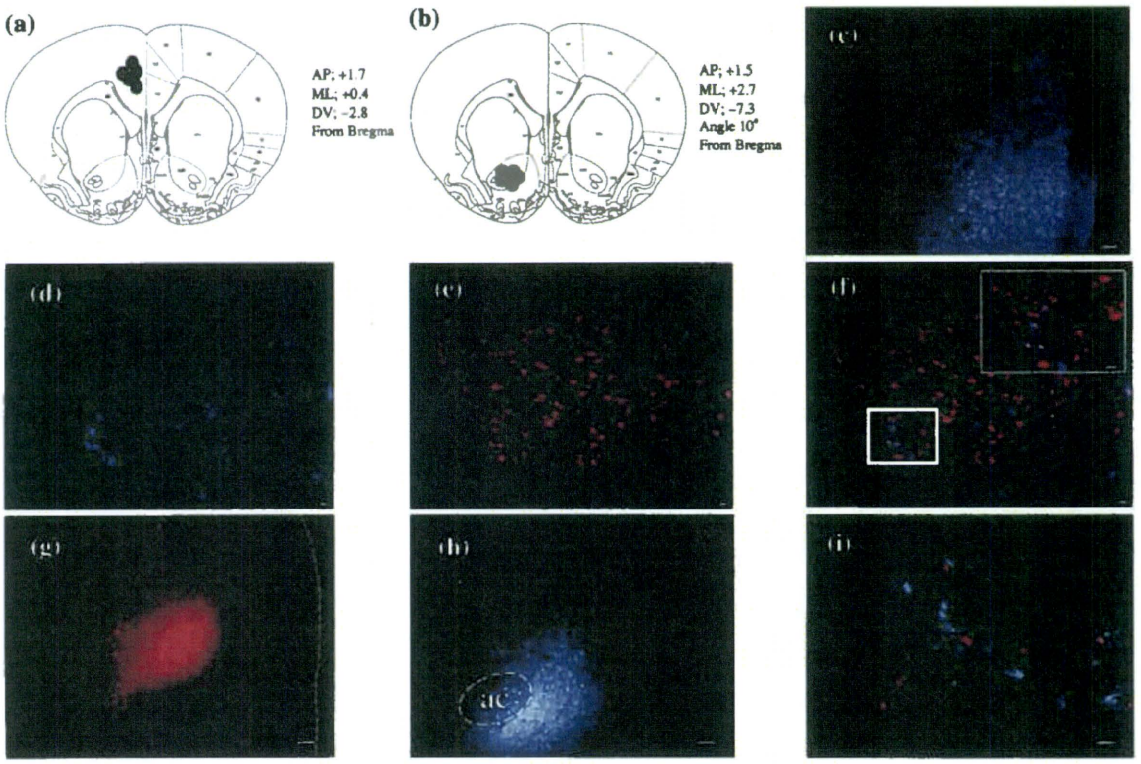

Figure 1 Projection of dopamine neurons from the ventral tegmental area (VTA) to the anterior cingulate cortex (ACG) and the distribution of cell bodies in the VTA projecting to the ACG or N.Acc of rats. (a–b) Schematic illustrations of the injection site (symbols) in the ACG (a) or N.Acc (b). (c) The image shows the extent of fluorogold (FG) diffusion at the injection site. (d) Cells in the VTA after the microinjection of FG into the ACG. (e) Tyrosine hydroxylase (TH)-IR was noted in the VTA. (f) Double-labelling experiments showed that FG-positive cells overlapped TH-positive cells in the VTA. (g) The extent of cholera toxin B diffusion at the injection site in the ACG. (h) The extent of FG diffusion at the injection site in the N.Acc. ac = anterior commissure. (i) Cells in the VTA after the microinjection of FG into the ACG and cholera toxin B into the N. Acc. Double-labelling experiments showed that FG-positive and cholera toxin B-positive cells did not overlap in the VTA. Scale bars, 50 μm

Table 1 Basal dialysate levels of dopamine and its metabolites in the nucleus accumbens or anterior cingulated cortex and the decrease in the contents of dopamine and its metabolites in the anterior cingulated cortex in desipramine-6-OHDA-treated rats.

	Dopamine	*DOPAC*	*HVA*
Brain area (nM)[a]			
Nucleus accumbens	0.8 ± 0.2	374.9 ± 86.2	109.7 ± 17.8
Cingulate cortex	0.2 ± 0.1*	19.2 ± 4.5**	24.3 ± 3.3**
Group (ng/g wet tissue)[b]			
Vehicle-saline	100.2 ± 0.901	34.7 ± 2.547	71.3 ± 1.678
Desipramine-6-OHDA	75.6 ± 0.396***	21.6 ± 0.514***	44.2 ± 0.450***

[a]Each value represents the mean ± SEM. The data were calculated as concentrations in the dialysates for five rats. *$P < 0.05$, **$P < 0.01$ versus dopamine, DOPAC or HVA in the N.Acc.

[b]Each value represents the mean ± SEM. The rats were killed four days after the microinjection of saline or 6-OHDA into the ACG. The data were calculated as dopamine and its metabolited contents in the ACG for four rats. The statistical significance of differences between groups was assessed with Student's *t*-test. ***$P < 0.001$ versus vehicle-saline.

of treatment, $F_{(1,88)} = 5.355$, $P < 0.05$; effect of time, $F_{(11,88)} = 2.567$, $P < 0.01$) (*$P < 0.05$, ***$P < 0.001$, saline versus DAMGO]. The dopamine and its metabolite levels were markedly increased by the injection of DAMGO compared with saline treatment in the N.Acc ($n = 5$) (Fig. 3f, g, h). Statistical analysis were performed with two-way ANOVA followed by Bonferroni test [dopamine: interaction between treatment and time: $F_{(11,88)} = 5.404$, $P < 0.001$; effect of treatment, $F_{(1,88)} = 8.963$, $P < 0.05$; effect of time, $F_{(11,88)} = 3.450$, $P < 0.001$; DOPAC: interaction between treatment and time: $F_{(11,88)} = 33.18$, $P < 0.001$; effect of treatment,

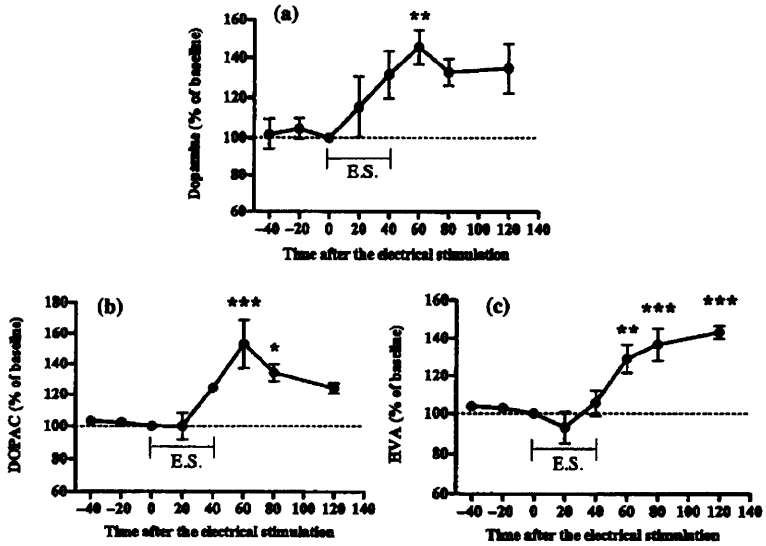

Figure 2 Change in the dialysate levels of dopamine and its metabolites induced by electrical stimulation (ES) in the rat VTA. (a–c) Effect of ES on the dialysate dopamine (a), DOPAC (b) and HVA (c) levels in the ACG in rats. The rats were subjected to electrical stimulation at time 0 for 40 minutes. The data are expressed as percentages of the corresponding baseline levels with SEM of the five rats. Dunnet test: $^{*}P<0.05$, $^{**}P<0.01$, $^{***}P<0.001$ versus 0 minute

$F_{(1,88)} = 50.84$, $P < 0.001$; effect of time, $F_{(11,88)} = 29.78$, $P < 0.001$; HVA: interaction between treatment and time: $F_{(11,88)} = 17.02$, $P < 0.001$; effect of treatment, $F_{(1,88)} = 24.11$, $P < 0.01$; effect of time, $F_{(11,88)} = 12.12$, $P < 0.001$) ($^{*}P < 0.05$, $^{**}P < 0.01$, $^{***}P < 0.001$, saline versus DAMGO].

Experiments III

Distribution of μ-opioid receptors in the VTA

We next investigated the distribution of MOR-IR in the VTA after the microinjection of FG into the ACG. FG-, MOR- or TH-labelled cells were detected in the VTA (Fig. 4a, b, c). A triple labelling experiment showed that MOR-IR in the VTA was detected on both TH- and non-TH-labelled neurons with a FG-positive reaction (Fig. 4e, f). Some MOR-labelled neurons with no FG reaction did not show TH-IR (Fig. 4g). Percentages of MOR, TH and FG labels, individually and in combination, in the VTA are shown in Fig. 4h.

Experiments IV

Role of VTA-ACG dopaminergic neurons in the acquisition and maintenance of the place preference induced by the μ-opioid receptor agonist

To investigate the involvement of VTA-ACG dopaminergic neurons in the induction of opioid reward, the rats were microinjected with 6-hydroxydopamine (6-OHDA) into the ACG after the s.c. injection of desipramine to specifically deplete dopamine. Pre-microinjection of 6-OHDA in combination with the s.c. administration of desipramine markedly decreased the basal levels of dopamine and its metabolites in the rat ACG ($^{***}P < 0.001$ versus vehicle-saline) ($n = 4$) (Table 1), whereas it failed to change the basal levels of dopamine and its metabolites in the N.Acc (Saline; $n = 6$, 6-OHDA; $n = 5$) [Dopamine: 88.8 ± 16.0 (% of control); DOPAC: 107.8 ± 15.7 (% of control); HVA: 98.0 ± 18.1 (% of control)]. The microinjection of 6-OHDA into the ACG after the treatment with desipramine did not affect NA and serotonin (5-HT) contents in the ACG [(NA: saline; 281.6 ± 11.6, 6-OHDA; 206.8 ± 14.7, NS, 5-HT: saline; 51.8 ± 1.4. 6-OHDA; 64.9 ± 5.1, NS (ng/g weight tissue)]. The injury of dopaminergic neurons, by 6-OHDA injection in the ACG, reduced TH-IR in the VTA ($^{*}P < 0.05$ versus saline) (Fig. 5a–c). In the CPP method, the microinjection of DAMGO into the VTA produced a dose-dependent place preference. The DAMGO-induced place preference was attenuated by the pre-microinjection of 6-OHDA into the ACG. The concentration-response line for the 6-OHDA-pre-treated group was shifted to the right compared with that for the saline-pre-treated group. The potency ratio of the place preference induced by DAMGO in saline-pre-treated group versus 6-OHDA-pre-treated group was 3.32 (saline: 0.3 nmol, $n = 7$; 1 nmol, $n = 6$; 3 nmol, $n = 8$, 6-OHDA: 1 nmol, $n = 8$; 3 nmol, $n = 6$; 9 nmol, $n = 6$) (Fig. 5d). The saline or the 6-OHDA pre-treated control rats failed to show the place preference (saline–saline: −36.9 ± 48.1, $n = 6$; 6-OHDA-saline: 22.7 ± 57.7, $n = 6$). Under these conditions, the 6-OHDA-pre-treated rats that produced the right shift of concentration–response line of the DAMGO-induced place preference showed extinction of the place preference at nine days after the final conditioning, whereas the place preference induced by the microinjection of DAMGO into the VTA in saline-pre-treated rats was maintained at nine days (Fig. 5e). Statistical analysis was performed with two-way ANOVA [saline; interaction between dose and day: $F_{(1,12)} = 0.6581$, NS; effect of dose, $F_{(1,12)} = 2.856$, NS;

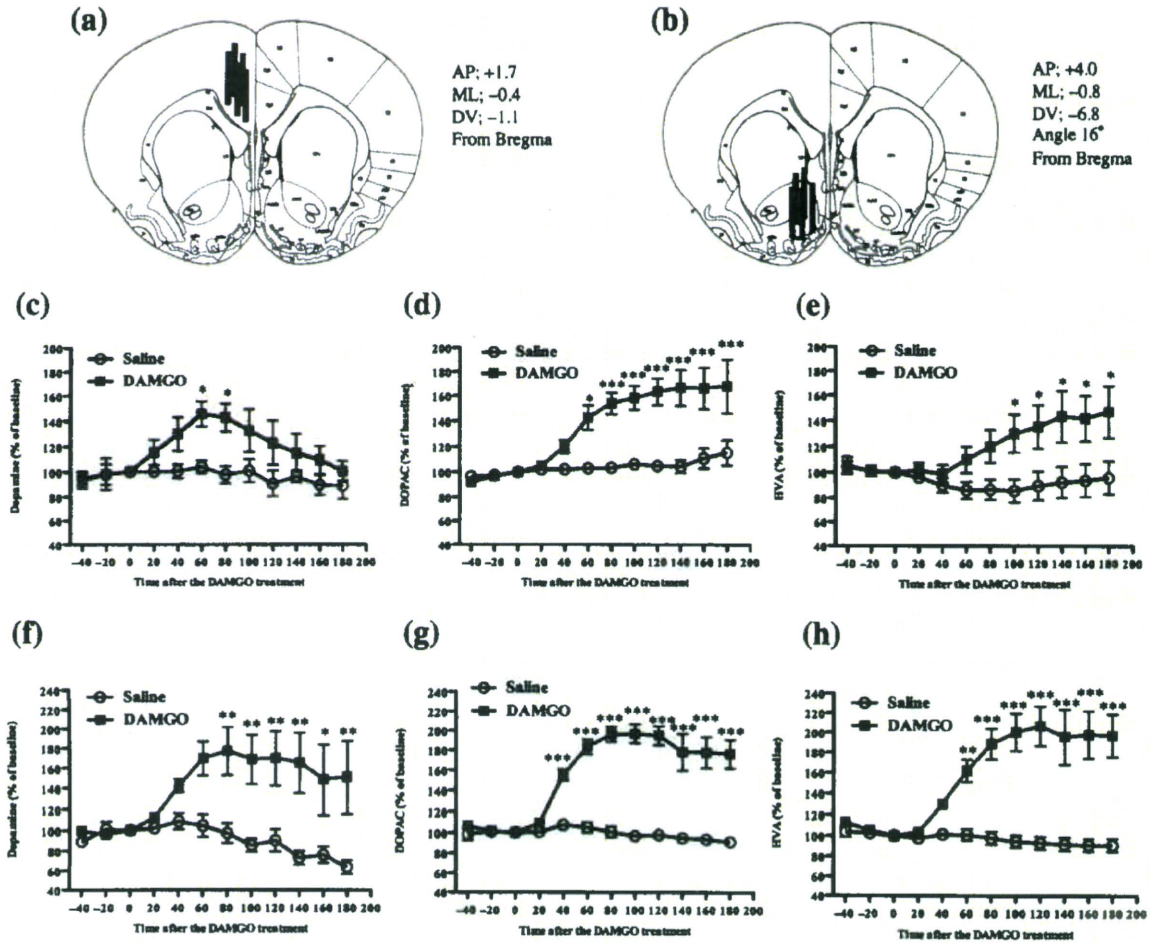

Figure 3 Change in the dialysate levels of dopamine and its metabolites induced by DAMGO administration into the VTA. (a–b) Schematic illustrations of the dialysis probe locations in the ACG (a) or N.Acc (b). (c–e) Effects of DAMGO administration into the VTA on the dialysate levels of dopamine (c) and its metabolites (d, e) in the ACG. After baseline fractions were collected, saline or DAMGO (1 nmol) was administered into the VTA at time 0 to evoke the release of dopamine. Data are expressed as percentages of the corresponding baseline levels with SEM for five rats. (f–h) Effects of DAMGO administration into the VTA on the dialysate levels of dopamine (f) and its metabolites (g, h) in the N.Acc. Data are expressed as percentages of the corresponding baseline levels with SEM for the five rats. Bonferroni test: $^{*}P < 0.05$, $^{**}P < 0.01$, $^{***}P < 0.001$, saline versus DAMGO

effect of day, $F_{(1,12)} = 0.02324$, NS, 6-OHDA; interaction between dose and day: $F_{(1,10)} = 0.9401$, NS; effect of dose, $F_{(1,10)} = 1.005$, NS; effect of day, $F_{(1,10)} = 14.57$, $P < 0.01$]. The saline- or 6-OHDA- pre-treated control rats failed to show the place preference at nine days after the final conditioning (saline–saline: -2.8 ± 45.1, $n = 6$; 6-OHDA-saline: 40.8 ± 36.6, $n = 6$). Furthermore, the 6-OHDA- pre-treated rats that received 23 mg/kg of morphine (i.p.), which exhibited the almost same score to that observed in the rats receiving 8 mg/kg of morphine (i.p.) showed early extinction after the post-test, whereas the saline-pre-treated rats that received 8 mg/kg of morphine failed to exhibit extinction of its place preference ($n = 6$). Statistical analysis was performed with two-way ANOVA [interaction between treatment and time: $F_{(3,30)} = 2.150$, NS; effect of treatment, $F_{(1,30)} = 5.284$, $P < 0.05$; effect of time, $F_{(3,30)} = 4.220$, $P < 0.05$] (Fig. 5f).

Experiments V

Activation of DARPP32 and CREB in the ACG of rats that maintained the μ-opioid-induced place preference

We next investigated whether the acquisition or maintenance of morphine-induced place preference could be associated with the phosphorylation of DARPP32 and CREB, which are the downstream of dopamine D1 receptor signalling in the ACG. The acquisition of morphine-induced place preference at 24 hours after the final conditioning was attenuated by pre-treatment of a

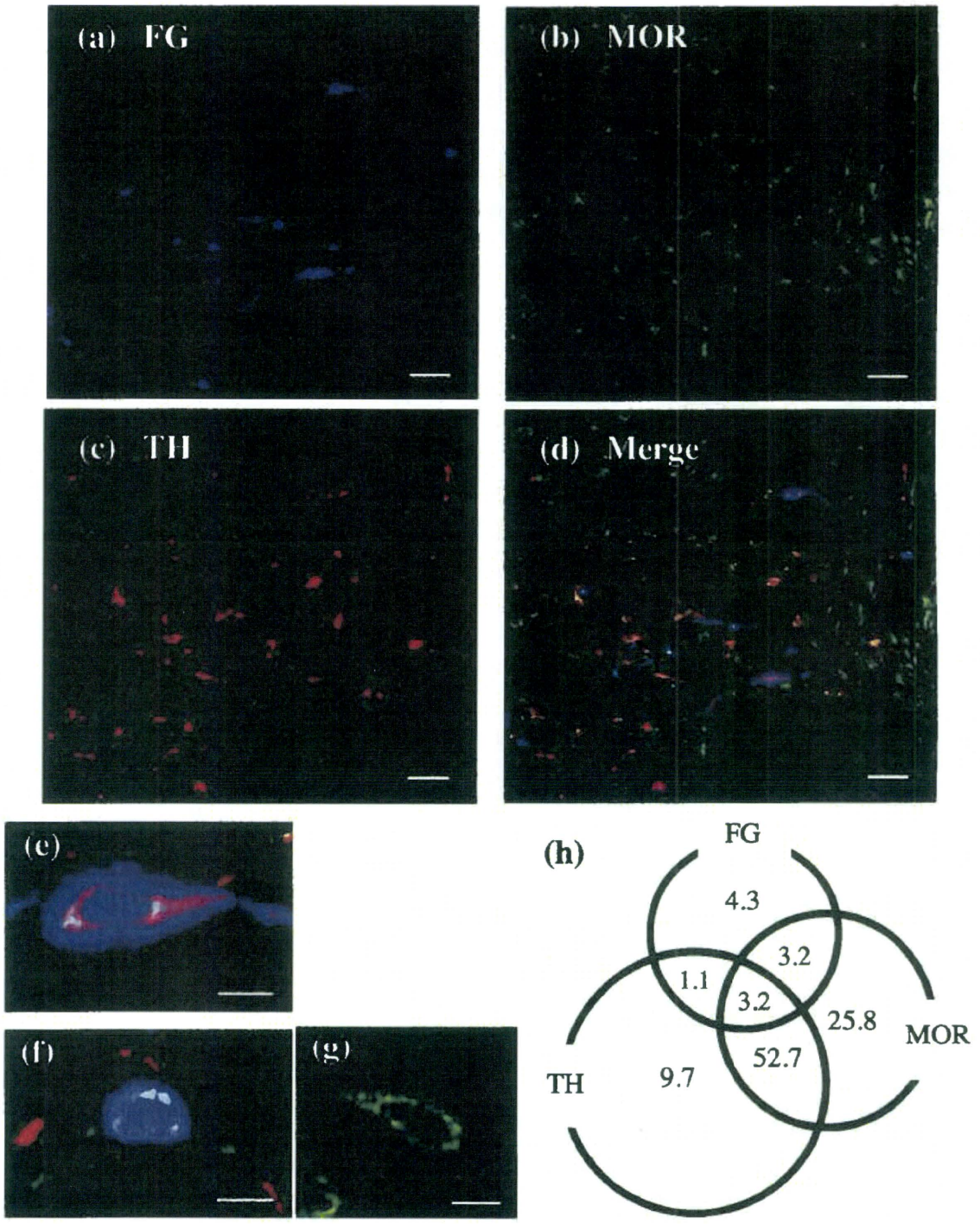

Figure 4 Characterization of μ-opioid receptors (MORs) in the VTA. (a) Cells in the VTA after the microinjection of FG into the ACG. (b) MOR-IR was noted in the VTA. (c) TH-IR was noted in the VTA. (d–g) (e–g: higher magnification) Triple-labelling experiments showed that MOR-IR in the VTA was present on both dopaminergic and non-dopaminergic neurons projecting to the ACG. Some of MOR-labelled neurons that did not project to the ACG did not show TH-IR. (h) Percentages of MOR-, TH- and FG-labels, individually and in combination, in the VTA. Scale bars, 50 μm (a–d), 10 μm (e–g)

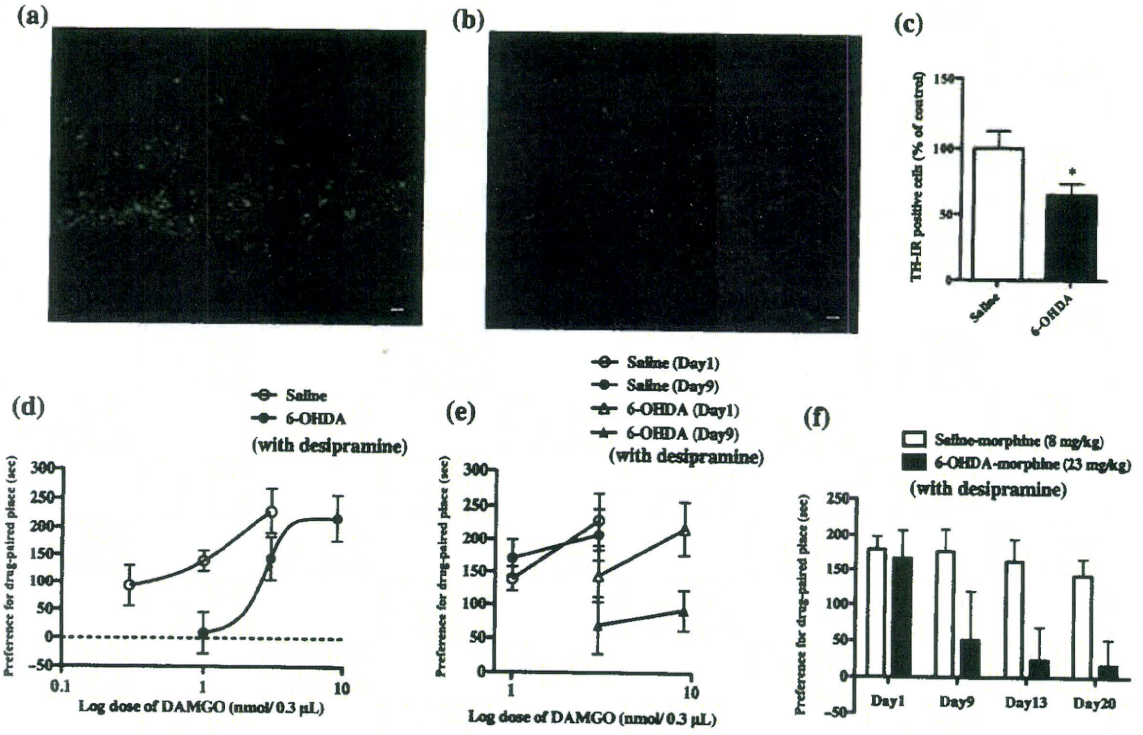

Figure 5 Involvement of dopamine neurons projecting from the VTA to the ACG in the DAMGO- or morphine-induced rewarding effect (a–b) Colour photomicrographs of immunofluorescent staining of TH-IR cells in the rat VTA following saline (a) or 6-OHDA (b) injection into the ACG. (c) Percent of TH-IR positive cells in the VTA of rats showing the saline or 6-OHDA injection into the ACG. Student's *t*-test: $^{*}P < 0.05$ versus saline. (d) DAMGO-induced place preference in the saline-pre-treated and 6-OHDA-pre-treated groups using the CPP assay are shown. The ordinate shows the preference for the drug-paired place, as defined by the post-conditioning test score minus the pre-conditioning test score in the drug treatment side. Each point represents the mean conditioning score with SEM of 6–8 rats. (e) Extinction of the DAMGO-induced place preference. Data show the conditioned place preference scores in saline- or 6-OHDA-pre-treated groups of 6–8 rats. Conditioning was performed for six days after the pre-conditioning test. The post-conditioning test was performed on the day after the final conditioning test (one day). To investigate the extinction of the DAMGO-induced place preference, a post-conditioning test was performed at nine days after the final conditioning test. (f) Extinction of the morphine-induced place preference. Data show the conditioned place preference scores in saline- or 6-OHDA-pre-treated groups of six rats. To investigate the extinction of the morphine-induced place preference, a post-conditioning test was performed on 9, 13, 20 days after the final conditioning test. Scale bars, 50 µm (a–b)

selective D1 receptor antagonist SCH23390. Furthermore, the maintenance of morphine-induced place preference at 10 days after the final conditioning also was suppressed by pre-treatment of SCH23390 (Fig. 6a, b). The levels of phosphorylated-DARPP32 (Thr34) and phosphorylated-CREB (Ser133) in the ACG at 24 hours after the final conditioning were not affected by morphine (Fig. 6c, e), whereas the morphine-induced place preference at 10 days after the final conditioning produced significant increases of phosphorylated-DARPP32 (Thr34) and phosphorylated-CREB (Ser133) levels in the ACG. The increases of these levels in the ACG were blocked by pre-treatment of SCH23390 (Fig. 6d, f). Statistical analysis was performed with one-way ANOVA followed by Bonferroni's multiple comparison test ($^{*}P < 0.05$, $^{**}P < 0.01$ versus saline–saline, $\#P < 0.05$, $\#\#P < 0.01$ versus saline–morphine).

DISCUSSION

The mPFC is composed of the infralimbic (IL), prelimbic (PL) (area CG3 of the ACG), dorsal and ventral anterior cingulate (areas CG1 and CG2 of the ACG) and medial precentral (frontal area 1) cortical areas (Paxinos & Watson 1998; Ongur & Price 2000). The mPFC receives dopaminergic efferents from the VTA, and thus is part of the mesocortical dopamine system, with the densest innervation occurring within the IL and PL regions (Thierry *et al.* 1973; Conde *et al.* 1995). Within the mPFC, the PL is the main source of afferents to the IL. Other projections to the IL originate from the hippocampus (CA1/subiculum), basolateral amygdala (BLA) and VTA. The PL receives projections from the IL, CG1 and CG2, hippocampus (CA1/subiculum), BLA and VTA. The primary sources of afferents to the CG1 and CG2 are con-

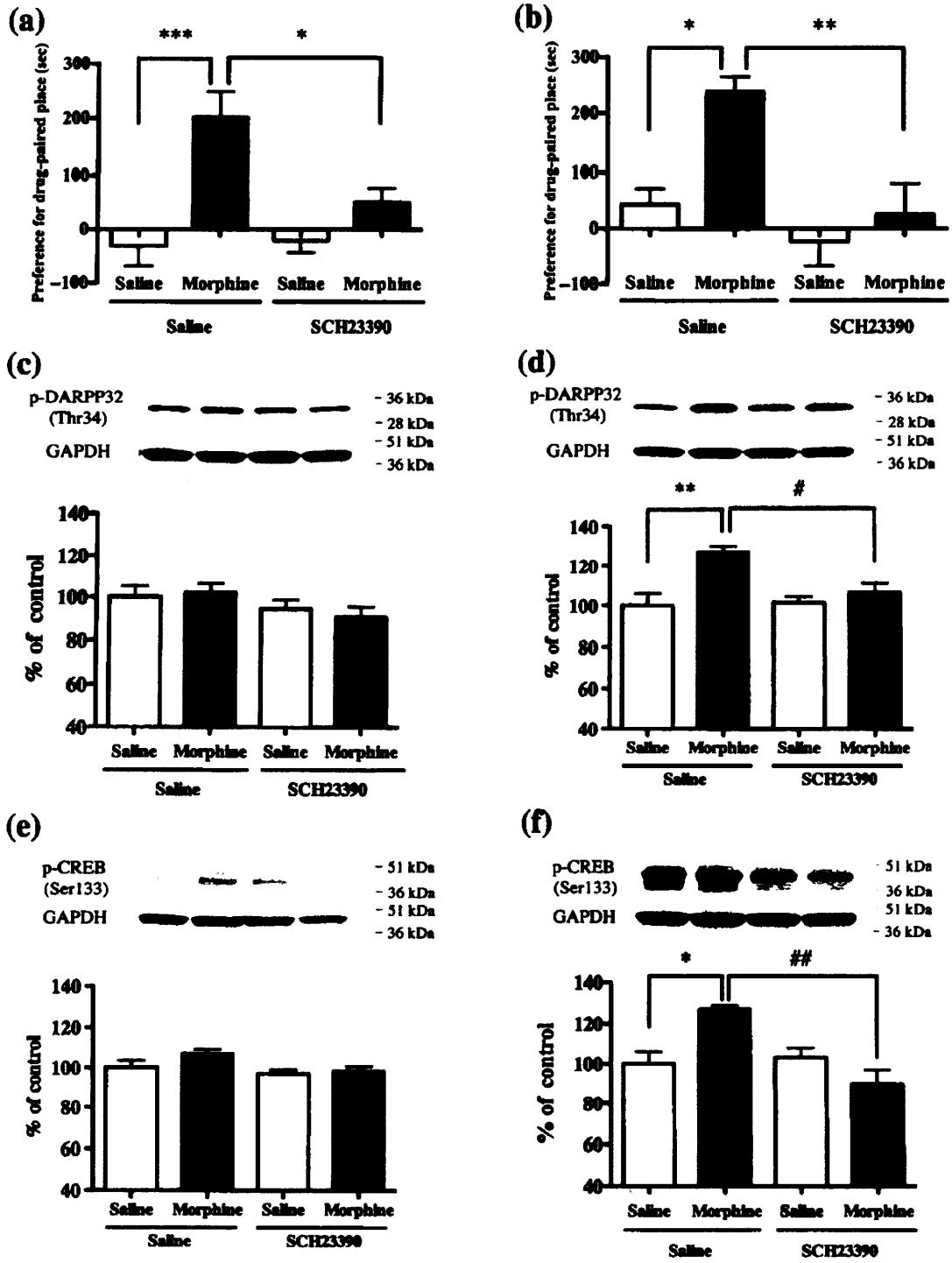

Figure 6 Changes in levels of phosphorylated DARPP32 (Thr34) or phosphorylated CREB (Ser133) in the ACG of rats that had acquired or maintained the morphine-induced place preference (a b) Change in the acquisition or maintenance of morphine-induced place preference at 24 hours (a) or 10 days (b) after the final conditioning. Data show the conditioned place preference scores in saline- or SCH23390-pre treated saline or morphine groups of six rats. (c–d) Change in the level of phosphorylated DARPP32 (Thr34) in lysate fractions of the ACG at 24 hours (c) or 10 days (d) after the final conditioning. (e–f) Change in the level of phosphorylated CREB (Ser133) in lysate fractions of the ACG at 24 hours (e) or 10 days (f) after the final conditioning. In the conditioning session, the rats were administered morphine (8 mg/kg, i.p.) 5 minutes after the pre-treatment of saline or SCH23390 (0.1 mg/kg, i.p.). Each column represents the mean with SEM of at least three independent experiments Bonferroni multiple comparison test: $^{*}P<0.05$, $^{**}P<0.01$ versus saline–saline, $\#P<0.05$, $\#\#P<0.01$ versus saline–morphine

sidered to be the PL, hippocampus (CA1/subiculum), BLA and VTA (Hoover & Vertes 2007). In the present study, several FG-positive VTA ACG projecting neurons in the VTA showed a TH-positive reaction, which suggested the existence of dopamine transmission in the ACG projecting from the VTA in the rat. In contrast, some of them exhibited a TH-negative reaction, which is supported by the finding that some GABAergic neurons in the VTA project to the mPFC (Carr & Sesack 2000). Furthermore, by using the retrograde tracer CTb as well as FG, we found that neurons that project from the VTA to the ACG exist independently and do not branch off from VTA–N.Acc projecting neurons. Interestingly, the ACG projects to the dorsal striatum, whereas the IL and PL project to the shell and core of the N.Acc, respectively (Berendse, Galis-de Graaf & Groenewegen 1992). We found that pre-microinjection of 6-OHDA into the ACG failed to change the basal levels of dopamine and its metabolites in the N.Acc. To further verify the dopaminergic neurons that project directly from the VTA to the ACG, we investigated whether the VTA-ACG dopaminergic pathway could be activated by the electrical stimulation of VTA cells. As a result, dopamine release with increased levels of its metabolites at the synaptic terminal in the ACG was increased by the electrical stimulation of VTA cells. These results provide physiological evidence for the existence of VTA–ACG dopaminergic projection.

In both the paranigral and parabrachial nuclei, which are the two major VTA subdivisions, MOR-labelling was observed within somata and proximal dendrites and was sometimes continuous with labelled neuronal somata (Garzon & Pickel 2001). In the present study, MOR was found at a high density in the VTA and was detected in both dopaminergic and non-dopaminergic VTA neurons projecting to the ACG. Some of the MOR-labelled neurons with no projecting to the ACG were also non-dopaminergic. In addition, in a preliminary study, we found that some of the MOR-labelled non-dopaminergic neurons in the VTA were GABAergic neurons (data not shown). These results are supported by a report that MOR agonists in the VTA affect dopaminergic transmission mainly indirectly through changes in the postsynaptic responsivity and/or presynaptic release from neurons containing other neurotransmitters, whereas MOR agonists also directly affect a small population of dopaminergic neurons expressing MOR on their dendrites in the VTA (Garzon & Pickel 2001).

We next investigated the possible release of dopamine in the ACG by the intra-VTA administration of a MOR agonist. The dopamine level at the synaptic terminal in the ACG was markedly increased by microinjection of DAMGO into the VTA. Microinjection of DAMGO into the VTA also produced a significant increase in the dopamine metabolites DOPAC and HVA, indicating that activation of MORs in the VTA by intra-VTA microinjection of DAMGO activates the VTA–ACG dopaminergic pathway in a depolarization-dependent manner.

The CPP procedure has been used extensively as an animal model for investigating the rewarding properties of drug-conditioned stimuli. The CPP procedure has also been used to investigate inhibitory effects on the acquisition (Shoblock, Wichmann & Maidment 2005; Esmaeili *et al.* 2009), consolidation (Alberini 2008; Esmaeili *et al.* 2009), expression (Shoblock *et al.* 2005; Esmaeili *et al.* 2009), extinction (Shoblock *et al.* 2005; Zhai *et al.* 2008), reinstatement (Shoblock *et al.* 2005; Popik, Wrobel & Bisaga 2006; Zhai *et al.* 2008) and reconsolidation (Alberini 2008). In the present study, the DAMGO-induced place preference was attenuated by the pre-microinjection of 6-OHDA, which destroys dopaminergic neurons, into the ACG. This finding is supported by a report that kainic acid lesions of the ACG prevent the acquisition of a morphine-induced place preference in mice (Hao *et al.* 2008). It was also reported that quinolinic acid lesions of the IL blocked the CPP induced by morphine, while lesions of the PL did not affect a morphine-induced CPP (Tzschentke & Schmidt 1999). Taken together, these findings suggest that the IL, CG1 and CG2 areas in the mPFC may be involved in the acquisition of μ-opioid-induced CPP.

More interestingly, we found here for the first time that rats that had been subjected to the ACG-microinjection of 6-OHDA failed to maintain μ-opioid-induced place preference in the early phase. Furthermore, the levels of phosphorylated DARPP32 (Thr34) and phosphorylated CREB (Ser133) in the ACG were increased in rats that maintained the μ-opioid-induced place preference, whereas the increases of these levels were almost abolished by pre-treatment of a selective dopamine D1 receptor antagonist. Although further examinations are needed to identify the role of VTA–ACG dopaminergic neurons in learning and memory, the present findings provide evidence that D1/DARPP32/CREB pathway in the ACG may be critical for the maintenance of a place preference induced by μ-opioids.

In conclusion, we have demonstrated here that dopamine in the ACG can be released by the activation of MORs in the VTA by MOR agonists, and the dopaminergic transmission that projects from the VTA to the ACG may be crucial for the acquisition and maintenance of the rewarding effects of μ-opioids. Furthermore, the activation of D1/DARPP32/CREB signalling in the ACG may be involved in the maintenance of the μ-opioid-induced place preference.

Acknowledgements

This work was supported by a Grant-in-Aid for Scientific Research and a research grant from the Ministry of Edu-

cation, Culture, Sports, Science and Technology of Japan. We thank Dr Keisuke Hashimoto, Mr Yasuhisa Kobayashi, Ms Sayuri Ishiwata, Mr Masaharu Furuya and Mr Natsuki Honda for their expert technical assistance.

Authors Contribution

MN and YM designed the experiments and wrote the manuscript. YM was responsible for most of the experimental work. KN contributed some of retrograde tracing and biochemical studies. MN performed biochemical experiments. ST, KN, KK, MA and MS conducted some of *in vivo* studies. MA and SI contributed some of biochemical experiments. KI and NK provided scientific and technical advice. TS supervised the overall projects. All authors discussed the results and commented on the manuscript.

References

Alberini CM (2008) The role of protein synthesis during the labile phases of memory: revisiting the skepticism. Neurobiol Learn Mem 89:234–246.

Alhaider AA (1991) Antinociceptive effect of ketanserin in mice: involvement of supraspinal 5-HT2 receptors in nociceptive transmission. Brain Res 543:335–340.

Almarestani L, Warers SM, Krause JE, Bennett GJ, Ribeiro-da-Silva A (2007) Morphological characterization of spinal cord dorsal horn lamina I neurons projecting to the parabrachial nucleus in the rat. J Comp Neurol 504:287–297.

Berendse HW, Galis-de Graaf Y, Groenewegen HJ (1992) Topographical organization and relationship with ventral striatal compartments of prefrontal corticostriatal projections in the rat. J Comp Neurol 316:314–347.

Berger B, Gaspar P, Verney C (1991) Dopaminergic innervation of the cerebral cortex: unexpected differences between rodents and primates. Trends Neurosci 14:21–27.

Carr DB, Sesack SR (2000) GABA-containing neurons in the rat ventral tegmental area project to the prefrontal cortex. Synapse 38:114–123.

Conde F, Maire-Lepoivre E, Audinat E, Crepel F (1995) Afferent connections of the medial frontal cortex of the rat. II. Cortical and subcortical afferents. J Comp Neurol 352:567–593.

Damasio AR (1995) On some functions of the human prefrontal cortex. Ann N Y Acad Sci 769:241–251.

Esmaeili B, Basseda Z, Gholizadeh S, Javadi Paydar M, Dehpour AR (2009) Tamoxifen disrupts consolidation and retrieval of morphine-associated contextual memory in male mice: interaction with estradiol. Psychopharmacology 204: 191–201.

Garzon M, Pickel VM (2001) Plasmalemmal mu-opioid receptor distribution mainly in nondopaminergic neurons in the rat ventral tegmental area. Synapse 41:311–328.

Hao Y, Yang J, Sun J, Qi J, Dong Y, Wu CF (2008) Lesions of the medial prefrontal cortex prevent the acquisition but not reinstatement of morphine-induced conditioned place preference in mice. Neurosci Lett 433:48–53.

Hoover WB, Vertes RP (2007) Anatomical analysis of afferent projections to the medial prefrontal cortex in the rat. Brain Struct Funct 212:149–179.

Jentsch JD, Redmond DE Jr, Elsworth JD, Taylor JR, Youngren KD, Roth RH (1997a) Enduring cognitive deficits and cortical dopamine dysfunction in monkeys after long-term administration of phencyclidine. Science 277:953–955.

Jentsch JD, Tran A, Le D, Youngren KD, Roth RH (1997b) Subchronic phencyclidine administration reduces mesoprefrontal dopamine utilization and impairs prefrontal cortical-dependent cognition in the rat. Neuropsychopharmacology 17:92–99.

Kelley AE, Berridge KC (2002) The neuroscience of natural rewards: relevance to addictive drugs. J Neurosci 22:3306–3311.

Kishi T, Tsumori T, Yokota S, Yasui Y (2006) Topographical projection from the hippocampal formation to the amygdala: a combined anterograde and retrograde tracing study in the rat. J Comp Neurol 496:349–368.

Koob GF (1992) Drugs of abuse: anatomy, pharmacology and function of reward pathways. Trends Pharmacol Sci 13:177–184.

Laemmli UK (1970) Cleavage of structural proteins during the assembly of the head of bacteriophage T4. Nature 227:680–685.

Merriam EP, Thase ME, Haas GL, Keshavan MS, Sweeney JA (1999) Prefrontal cortical dysfunction in depression determined by Wisconsin Card Sorting Test performance. Am J Psychiatry 156:780–782.

Nestler EJ (2001) Molecular basis of long-term plasticity underlying addiction. Nat Rev Neurosci 2:119–128.

Ongur D, Price JL (2000) The organization of networks within the orbital and medial prefrontal cortex of rats, monkeys and humans. Cereb Cortex 10:206–219.

Paxinos G, Watson C (1998) The Rat Brain in Stereotaxic Coordinates, 4th edn. New York: Academic Press.

Peoples LL (2002) Neuroscience. Will, anterior cingulate cortex, and addiction. Science 296:1623–1624.

Pierce RC, Kumaresan V (2006) The mesolimbic dopamine system: the final common pathway for the reinforcing effect of drugs of abuse? Neurosci Biobehav Rev 30:215–238.

Popik P, Wrobel M, Bisaga A (2006) Reinstatement of morphine-conditioned reward is blocked by memantine. Neuropsychopharmacology 31:160–170.

Puumala T, Sirvio J (1998) Changes in activities of dopamine and serotonin systems in the frontal cortex underlie poor choice accuracy and impulsivity of rats in an attention task. Neuroscience 83:489–499.

Rushworth MF, Walton ME, Kennerley SW, Bannerman DM (2004) Action sets and decisions in the medial frontal cortex. Trends Cogn Sci 8:410–417.

Schweimer J, Saft S, Hauber W (2005) Involvement of catecholamine neurotransmission in the rat anterior cingulate in effort-related decision making. Behav Neurosci 119:1687–1692.

Shoblock JR, Wichmann J, Maidment NT (2005) The effect of a systemically active ORL-1 agonist, Ro 64-6198, on the acquisition, expression, extinction, and reinstatement of morphine conditioned place preference. Neuropharmacology 49:439–446.

Steen PA, Mason M, Pham L, Lefebvre Y, Hickmott PW (2007) Axonal bias at a representational border in adult rat somatosensory cortex (S1). J Comp Neurol 500:634–645.

Suzuki T, Masukawa Y, Misawa M (1990) Drug interactions in the reinforcing effects of over-the-counter cough syrups. Psychopharmacology 102:438–442.

Tallarida RJ, Porreca F, Cowan A (1989) Statistical analysis of drug–drug and site–site interactions with isobolograms. Life Sci 45:947–961.

Thierry AM, Blanc G, Sobel A, Stinus L, Golwinski J (1973) Dopaminergic terminals in the rat cortex. Science 182:499–501.

Tzschentke TM, Schmidt WJ (1999) Functional heterogeneity of the rat medial prefrontal cortex: effects of discrete subarea-specific lesions on drug-induced conditioned place preference and behavioural sensitization. Eur J Neurosci 11:4099–4109.

Tzschentke TM, Schmidt WJ (2000) Differential effects of discrete subarea-specific lesions of the rat medial prefrontal cortex on amphetamine- and cocaine-induced behavioural sensitization. Cereb Cortex 10:488–498.

Ventura R, Alcaro A, Puglisi-Allegra S (2005) Prefrontal cortical norepinephrine release is critical for morphine-induced reward, reinstatement and dopamine release in the nucleus accumbens. Cereb Cortex 15:1877–1886.

Walton ME, Bannerman DM, Alterescu K, Rushworth MF (2003) Functional specialization within medial frontal cortex of the anterior cingulate for evaluating effort-related decisions. J Neurosci 23:6475–6479.

Weinberger D (1995) Neurodevelopmental perspectives on schizophrenia. In: Bloom FE, Kupfer DJ, eds. The Fourth Generation of Progress, pp. 1171–1183. New York: Raven.

Williams GV, Goldman-Rakic PS (1995) Modulation of memory fields by dopamine D1 receptors in prefrontal cortex. Nature 376:572–575.

Wise SP, Murray EA, Gerfen CR (1996) The frontal cortex-basal ganglia system in primates. Crit Rev Neurobiol 10:317–356.

Zhai H, Wu P, Xu C, Liu Y, Lu L (2008) Blockade of cue- and drug-induced reinstatement of morphine-induced conditioned place preference with intermittent sucrose intake. Pharmacol Biochem Behav 90:404–408.

別紙４

研究成果の刊行に関する一覧表

書籍

著者氏名	論文タイトル名	書籍全体の編集者名	書　籍　名	出版社名	出版地	出版年	ページ

雑誌

発表者氏名	論文タイトル名	発表誌名	巻号	ページ	出版年
Dobashi T, Nishino T, et al.	Valproate attenuates the development of morphine antinociceptive tolerance.	Neurosci Lett	149	412-413	2010
Tagaito Y, Nishino T. et al.	Sitting posture decreases collapsibility of the passive pharynx in anesthetized paralyzed p	Anethesiology	113	812-818	2010
Nishino T	Dyspnea and its interaction with pain.	J Anesth	25	157-161	2011
西野　卓	麻酔管理に役立つ呼吸生理。	麻酔	59増刊	S147-S15	2010

Neuroscience Letters 485 (2010) 125–128

Contents lists available at ScienceDirect

Neuroscience Letters

journal homepage: www.elsevier.com/locate/neulet

Valproate attenuates the development of morphine antinociceptive tolerance

Tamae Dobashi, Serabi Tanabe, Hisayo Jin, Takashi Nishino, Tomohiko Aoe*

Department of Anesthesiology, Chiba University Graduate School of Medicine, 1-8-1 Inohana, Chuo-ku, Chiba 260-8670, Japan

ARTICLE INFO

Article history:
Received 9 July 2010
Received in revised form 27 August 2010
Accepted 28 August 2010

Keywords:
Morphine tolerance
Mood stabilizer
Opioid
Glycogen synthase kinase

ABSTRACT

Morphine is a potent opioid analgesic. Repeated administration of morphine induces tolerance, thus reducing the effectiveness of analgesic treatment. Although some adjuvant analgesics can increase morphine analgesia, the precise molecular mechanism behind their effects remains unclear. Opioids bind to the mu opioid receptor (MOR). Morphine tolerance may be derived from alterations in the intracellular signal transduction after MOR activation. Chronic morphine treatment activates glycogen synthase kinase 3β (GSK3β), whose inhibition diminishes morphine tolerance. Valproate is widely prescribed as an anticonvulsant and a mood stabilizer for bipolar disorders because it increases the amount of γ-aminobutyric acid (GABA) in the central nervous system. Although the activation of GABAergic neurons may be responsible for the chief pharmacologic effect of valproate, recent studies have shown that valproate also suppresses GSK3β activity. We examined the effect of valproate on the development of morphine antinociceptive tolerance in a mouse model of thermal injury. Mice were treated with morphine alone or with morphine and valproate twice daily for 5 days. The resulting antinociceptive effects were assessed using a hot plate test. While mice treated with morphine developed tolerance, co-administration of valproate attenuated the development of tolerance and impaired the activation of GSK3β in mice brains. Valproate alone did not show analgesic effects; nevertheless, it functioned as an adjuvant analgesic to prevent the development of morphine tolerance. These results suggest that the modulation of GSK3β activity by valproate may be useful and may play a role in the prevention of morphine tolerance.

Morphine is a potent opioid analgesic that is widely used for acute and chronic pain control [24]. Repeated administration of morphine induces tolerance, which reduces its effectiveness as an analgesic agent. Opioids bind to the mu opioid receptor (MOR) to activate various signaling molecules through heterotrimeric guanine nucleotide-binding proteins (G proteins). Chronic morphine tolerance may arise from adaptations in the intracellular signal transduction after MOR activation, as morphine does not effectively induce MOR phosphorylation or internalization [9]. Persistent activation of MOR on the cell surface may cause altered signal transduction including changes in MOR-coupled G proteins from Giα to Gsα [5], increased activity of protein kinase C [11], and upregulation of *N*-methyl-D-aspartate receptor signaling [26]. Chronic morphine treatment also activates the cyclin-dependent kinase 5-glycogen synthase kinase-3β (GSK3β) signaling pathway, while inhibition of this pathway diminishes morphine tolerance and restores the efficacy of analgesic in rat [20] and mouse models [7].

Valproate is widely prescribed as an anticonvulsant and a mood stabilizer for bipolar disorders. It increases the amount of γ-aminobutyric acid (GABA) in the central nervous system [18]. Although the activation of GABAergic neurons may be responsible for the central pharmacologic effect of valproate, recent studies have shown that valproate also suppresses the activity of GSK3β [2,14]. Since valproate use is frequent in clinical discourse, we examined the effect of valproate as an inhibitor of GSK3β on the development of morphine antinociceptive tolerance in a mouse model of thermal injury.

All animal experimental procedures were in accordance with a protocol approved by the Institutional Animal Care Committee of Chiba University, Chiba, Japan. C57BL/6 male mice (22–27 g; aged 10–15 weeks; 69 mice) were used. All mice were provided with food and water *ad libitum* before the experiment.

The following reagents were used: sodium valproate (Sigma Chemical Co., Irvine, UK), morphine hydrochloride (Takeda Pharmaceutical Co., Tokyo, Japan), and SB216763 (Biomol International, Plymouth Meeting, PA, USA). The following antibodies were used: rabbit polyclonal antibody against MOR-1 (Chemicon, Temecula, CA, USA), mouse monoclonal antibody (mAb) against phospho-GSK3β (Tyr279/Tyr216) (Upstate Biotechnology, Chicago, IL, USA), Cy-3-conjugated donkey antibody against rabbit IgG, and Cy-2-conjugated donkey antibody against mouse IgG (Jackson Immunoresearch Laboratories, West Grove, PA, USA).

Abbreviations: MOR, mu opioid receptor; G proteins, heterotrimeric guanine nucleotide-binding proteins; GSK3β, glycogen synthase kinase 3β; GABA, γ-aminobutyric acid.

* Corresponding author. Tel.: +81 43 226 2573; fax: +81 43 226 2156.
E-mail address: taoe@faculty.chiba-u.jp (T. Aoe).

0304-3940/$ – see front matter © 2010 Elsevier Ireland Ltd. All rights reserved.
doi:10.1016/j.neulet.2010.08.084

A hot plate test was carried out to assess the effects of a pharmacologic agent on the thermal nociceptive threshold of mice. Mice were placed on a 54.5 C hot plate (Socrel hot-plate model DS37, Ugo Basile, Italy). The response latency to either a hind paw lick or a jump was recorded. In the absence of a response, the animals were removed from the hot plate after 60 s to avoid tissue injuries, and a 60 s latency was assigned as the response. Before drug administration, the hot plate latency was measured 3 times, and the average of the second and third measurements was used as the pre-drug response latency at 0 min. The hot plate latency was also measured at 5, 15, 30, 45, and 60 min following intraperitoneal drug injection. Each reagent was dissolved in 100 μl saline for intraperitoneal injection. To confirm analgesia with morphine, the hot plate latency was measured at 5, 15, 30, 45, and 60 min after a single intraperitoneal injection with morphine (20 mg/kg, $n = 25$). To obtain control data, mice were injected with the vehicle (saline, $n = 2$) or valproate (150 mg/kg; $n = 5$) twice a day for 5 days, and the hot plate tests were performed on day 5 after the pharmacological agents were administered intraperitoneally. To evaluate the effect of valproate on morphine analgesia, 20 mg/kg morphine alone ($n = 12$) or morphine with valproate (50, 150, 300 mg/kg; $n = 5$, 14, 5, respectively) were administered intraperitoneally twice a day for 5 days. On day 5, more than 6 h after drug administration, mice were administered 20 mg/kg of morphine and then subjected to the hot plate test.

To analyze the effects of these drugs on animal performance in the hot plate test, the %MPE was calculated, where %MPE = ([post-drug maximum response latency − pre-drug response latency]/[cut-off time {60 s} − pre-drug response latency]) × 100. The post-drug maximum response latency was defined as the single longest response latency during the entire time course of the hot plate test. A higher %MPE represented a better analgesic effect.

Mice were deeply anesthetized with pentobarbital (Dainippon Sumitomo Pharma, Osaka, Japan) and fixed by transcardial perfusion with 4% paraformaldehyde in phosphate-buffered saline (PBS). Their brains were further immersion-fixed for 12 h in 4% paraformaldehyde at 4 C. After fixation, the brains were dehydrated by immersing in increasing concentrations of ethanol, and subsequently embedded in paraffin wax. For immunofluorescence, sections (8 μm) were incubated with 10% normal goat or bovine serum in PBS for 30 min to block nonspecific antibody binding and then incubated with a primary antibody in PBS for 1 h at room temperature. The sections were rinsed with PBS and then incubated with a mixture of Cy-3-conjugated anti-rabbit IgG and Cy-2-conjugated anti-mouse IgG in PBS for 1 h at room temperature. Subsequently, the sections were rinsed with PBS and mounted on glass slides with Perma Fluor (Immunon, Pittsburgh, PA, USA). Immunolocalization was observed with a fluorescence microscope using FITC/rhodamine filters and Plan-Neofluar 20× and 40× NA 0.75 objectives (Axiovert 200 M; Carl Zeiss, Oberkochen, Germany). The brightness and contrast were optimized using AxioVision 4.4 software (Carl Zeiss), and immunofluorescence images were captured with a digital camera (AxioCam MRm, Carl Zeiss). The mean grey values of cells with the background subtraction were used for densitometry.

To compare the hot plate %MPE, latencies, and other values between groups, one-way or two-way ANOVA was used followed by the Bonferroni post hoc test (GraphPad Prism 4.0, GraphPad Software, San Diego, CA, USA).

We evaluated analgesia induced with administration of a single dose of morphine (20 mg/kg) administration in our mice model with the hot plate test (Fig. 1A). The response latencies reached the 60 s cut-off point 30 min after injection. The response latencies of the valproate injection group and the saline control group (NS) did not differ significantly (Fig. 1A). Thus, valproate alone did not affect the nociceptive threshold of mice.

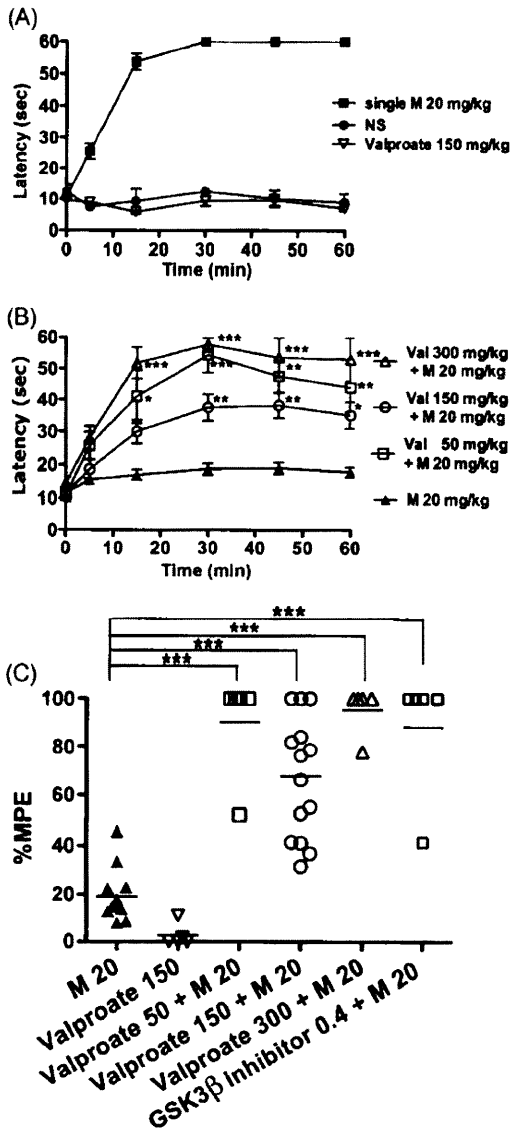

Fig. 1. Valproate attenuated the development of morphine tolerance. (A) The graph represents the latent responses (0–60 s) of mice administered morphine once (single M), saline twice a day for 5 consecutive days (NS), or 150 mg/kg of valproate twice a day for 5 consecutive days (mean ± SEM). (B) The graph represents the latent responses (0–60 s) of mice administered morphine alone (M, $n = 12$), 50 mg/kg of valproate and morphine, 150 mg/kg valproate and morphine, and 300 mg/kg valproate and morphine twice a day for 5 consecutive days (mean ± SEM; $^{*}P < 0.05$; $^{**}P < 0.01$; $^{***}P < 0.001$, two-way ANOVA with the Bonferroni post hoc test). (C) The distribution of %MPE after the repetitive drug treatment for 5 days. The mean %MPEs of the mice that received valproate and morphine were significantly greater than those of mice treated with morphine alone. The mean %MPE of mice receiving GSK3β inhibitor (0.4 mg/kg of SB216763) and morphine ($n = 5$) was also significantly greater than that of mice treated with morphine alone ($^{***}P < 0.001$, one-way ANOVA with the Bonferroni post hoc test).

Subsequently, to evaluate the effect of valproate on morphine tolerance, mice were administered morphine alone or a combination of morphine and valproate intraperitoneally twice a day for 5 consecutive days. On day 5, more than 6 h after the drug administration, mice were administered morphine alone (20 mg/kg) and then subjected to the hot plate test (Fig. 1B). We found that the response latencies were significantly reduced, indicating that morphine tolerance was induced by repeatedly injecting morphine (Fig. 1B, M20). On the other hand, the latent responses of mice co-administered valproate and morphine were significantly longer

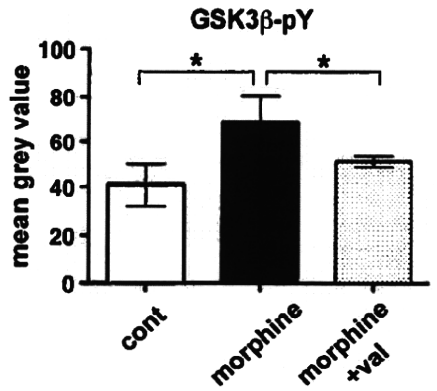

Fig. 2. GSK3β activation is reduced in mice administered valproate and morphine. Wild-type mice were injected with 20 mg/kg morphine alone (morphine), 150 mg/kg valproate and morphine (morphine+val), or saline (cont) twice a day for 5 days. The brains were sectioned and double-immunostained with anti-phospho-GSK3β (Tyr216) and anti-MOR. Based on densitometric analysis, MOR-immunopositive neurons in the PAG matter of mice injected with morphine alone showed a significantly greater enhancement of expression of tyrosine-phosphorylated GSK3β after chronic morphine treatment than mice treated with morphine and valproate (arbitrary unit; $n=10$; mean ± SD; $^*P<0.05$, one-way ANOVA with the Bonferroni post hoc test). A representative immunohistochemistry result is shown in Supplementary Fig. 1.

than those of mice that received morphine alone at 15, 30, 45, and 60 min after drug administration (Fig. 1B).

The mean %MPEs of mice co-administered valproate and morphine were significantly greater than that of mice administered morphine alone (Fig. 1C). These results indicated that valproate alone does not provide analgesic effect, but it does inhibit the development of morphine antinociceptive tolerance.

GSK3β inhibition by specific inhibitors such as SB216763 and (2′Z, 3′E)-6-bromoindirubin-3′-oxime diminishes the development of morphine tolerance in rats after chronic intrathecal morphine treatment [20]. In addition, we verified that GSK3β inhibition by SB216763 suppressed the development of morphine antinociceptive tolerance in our mouse models [7]. Furthermore, we co-administered SB216763 (0.4 mg/kg) and morphine (20 mg/kg) twice a day for 5 days. The response latencies of mice following this co-administration were significantly longer than those of control mice that received morphine alone following the last morphine injection on day 5. The mean %MPE of mice that received both SB216763 (0.4 mg/kg) and morphine was significantly greater than that of mice treated with morphine alone on day 5 (Fig. 1C). SB216763 alone did not provide analgesic effect [7]. Thus, the inhibition of GSK3β prevented the development of morphine tolerance.

Since morphine and valproate were injected intraperitoneally, both spinal and supraspinal neurons might have been affected. Neurons exhibiting MOR expression in the periaqueductal gray (PAG) matter contribute to morphine tolerance [1,19,27]. After chronic intraperitoneal injection of morphine alone or the combination of morphine with valproate for 5 days, mouse brains were sectioned and double-immunostained with antibodies against MOR and tyrosine-phosphorylated GSK3β. We examined 3 mice in each group. Mice that were administered the combination of morphine and valproate remained sensitive to morphine analgesia with 100% MPE (mean). On the other hand, mice administered morphine alone revealed diminished analgesia with 15.3% MPE (mean). MOR-immunopositive neurons in the PAG region of mice that were injected morphine alone showed a significantly greater enhancement of tyrosine-phosphorylated GSK3β expression than those of mice injected with morphine and valproate (Fig. 2 and Supplementary Fig. 1).

These observations suggest that chronic MOR stimulation by repetitive morphine injections may activate GSK3β, which might be related to the development of morphine tolerance. Mice injected with morphine and valproate remained morphine-sensitive, and the inhibition of GSK3β by valproate may have thus contributed to the attenuation of the development of morphine tolerance.

This study shows that systemic administration of valproate suppressed the development of morphine antinociceptive tolerance in a mouse model. Although administration of valproate alone did not exhibit an analgesic effect, it functioned as an adjuvant analgesic to prevent the development of morphine tolerance.

Chronic morphine administration may alter the signal transduction through persistent MOR activation. We thus examined the role of GSK3β as a ventral signaling molecule in the MOR signaling pathway. GSK3β is a serine/threonine kinase that plays critical roles in diverse intracellular signaling systems [12]. Its kinase activity is inactivated by the phosphorylation of Ser9, while the same is enhanced by the dephosphorylation of Ser9 and the phosphorylation of Tyr216. The p90 ribosomal S6 kinase [25], Akt [6], protein kinase C [10], and protein kinase A [8] have been demonstrated to phosphorylate GSK3β at Ser9. While acute activation of MOR inactivates GSK3β by the phosphorylation of Ser9 through the PI3K/Akt pathway [12], the chronic activation of MOR may activate GSK3β, which is associated with the development of morphine tolerance [20]. ZAK1 [15], Fyn tyrosine kinases [16], and transient increases in intracellular Ca^{2+} [13] have been reported to activate GSK3β by inducing phosphorylation of Tyr216; however, the regulatory mechanism for the activation of GSK3β remains uncertain in comparison to the mechanism responsible for its inactivation. Although the precise molecular mechanism of MOR-mediated GSK3β activation remains uncertain, it is hypothesized that morphine administration induces an elevation in cytosolic Ca^{2+} levels by both an influx of extracellular Ca^{2+} and a release of Ca^{2+} from its intracellular stores [21]. Persistent activation of MOR on the cell surface may cause an upregulation of *N*-methyl-D-aspartate receptor signaling [26], leading to an influx of extracellular Ca^{2+}, which would possibly lead to the activation of GSK3β.

Activation of MOR triggers signal transduction, leading to the induction and activation of transcriptional factors such as activator protein-1 (AP-1), which may cause alterations of gene expression related to the development of tolerance and dependence. Acute treatment of MOR with morphine stimulates AP-1 DNA-binding activity, while chronic treatment normalizes it [3]. FosB−/− mice, as compared to fosB+/+ mice, developed enhanced tolerance to morphine-induced analgesia [23]. Thus, AP-1 seems to be involved in the development of morphine tolerance. GSK3β has been reported to be a negative regulator of growth factor-induced activation of the c-Jun *N*-terminal kinase [17], and the phosphorylation of recombinant human c-Jun proteins in vitro by GSK3β also decreases its DNA-binding activity [4]. On the other hand, the inhibition of GSK3β appears to be required for effective morphine analgesia because co-administration of morphine and GSK3β inhibitors was found to prevent the development of morphine tolerance, as shown in previous studies [7,20]. Although the precise mechanism by which the activation of GSK3β causes morphine tolerance is unclear, the activation of GSK3β possibly leads to the decrease in the DNA-binding activity of AP-1 as well as the development of morphine tolerance.

In this study, we did not observe any dose-dependent effect for valproate when 50–300 mg/kg of valproate was administered twice a day for 5 days. Although valproate concentrations were not evaluated, we believe that concentrations less than 50 mg/kg might also be effective in preventing the development of morphine antinociceptive tolerance. In the clinical setting, up to 1200 mg/day of valproate is prescribed; therefore, approximately 10 mg/kg of valproate should be administered twice a day. Although the dosage

used in our mouse experiments did not drastically differ from those used in the human clinical setting, a smaller dose of valproate should be tested for future clinical applications.

This study has demonstrated that the co-administration of valproate with morphine suppressed the development of morphine tolerance. Since valproate has multiple biological effects [22], inactivation of GSK3β as well as GABAergic action may contribute to the attenuation of morphine tolerance. Further investigation is required to elucidate the relationship between morphine tolerance and GSK3β signaling. The modulation of GSK3β activity by valproate may be a potentially viable clinical application for preventing morphine tolerance.

Acknowledgement

This work was supported by Grants-in-Aids for Science Research from the Ministry of Education, Culture, Sports, Science, and Technology of Japan to T.D and T.A.

Appendix A. Supplementary data

Supplementary data associated with this article can be found, in the online version, at doi:10.1016/j.neulet.2010.08.084.

References

[1] E.E. Bagley, B.C. Chieng, M.J. Christie, M. Connor, Opioid tolerance in periaqueductal gray neurons isolated from mice chronically treated with morphine, Br. J. Pharmacol. 146 (2005) 68–76.
[2] A.M. Bielecka, E. Obuchowicz, Antiapoptotic action of lithium and valproate, Pharmacol. Rep. 60 (2008) 771–782.
[3] W. Bilecki, A. Wawrzczak-Bargiela, R. Przewlocki, Activation of AP-1 and CRE-dependent gene expression via mu-opioid receptor, J. Neurochem. 90 (2004) 874–882.
[4] W.J. Boyle, T. Smeal, L.H. Defize, P. Angel, J.R. Woodgett, M. Karin, T. Hunter, Activation of protein kinase C decreases phosphorylation of c-Jun at sites that negatively regulate its DNA-binding activity, Cell 64 (1991) 573–584.
[5] S. Chakrabarti, A. Regec, A.R. Gintzler, Biochemical demonstration of mu-opioid receptor association with Gsalpha: enhancement following morphine exposure, Brain Res. Mol. Brain Res. 135 (2005) 217–224.
[6] D.A. Cross, D.R. Alessi, P. Cohen, M. Andjelkovich, B.A. Hemmings, Inhibition of glycogen synthase kinase-3 by insulin mediated by protein kinase B, Nature 378 (1995) 785–789.
[7] T. Dobashi, S. Tanabe, H. Jin, N. Mimura, T. Yamamoto, T. Nishino, T. Aoe, BiP, an endoplasmic reticulum chaperone, modulates the development of morphine antinociceptive tolerance, J. Cell Mol. Med., in press.
[8] X. Fang, S.X. Yu, Y. Lu, R.C. Bast Jr., J.R. Woodgett, G.B. Mills, Phosphorylation and inactivation of glycogen synthase kinase 3 by protein kinase A, Proc. Natl. Acad. Sci. U.S.A. 97 (2000) 11960–11965.
[9] A.K. Finn, J.L. Whistler, Endocytosis of the mu opioid receptor reduces tolerance and a cellular hallmark of opiate withdrawal, Neuron 32 (2001) 829–839.
[10] N. Goode, K. Hughes, J.R. Woodgett, P.J. Parker, Differential regulation of glycogen synthase kinase-3 beta by protein kinase C isotypes, J. Biol. Chem. 267 (1992) 16878–16882.
[11] V. Granados-Soto, I. Kalcheva, X. Hua, A. Newton, T.L. Yaksh, Spinal PKC activity and expression: role in tolerance produced by continuous spinal morphine infusion, Pain 85 (2000) 395–404.
[12] C.A. Grimes, R.S. Jope, The multifaceted roles of glycogen synthase kinase 3beta in cellular signaling, Prog. Neurobiol. 65 (2001) 391–426.
[13] J.A. Hartigan, G.V. Johnson, Transient increases in intracellular calcium result in prolonged site-selective increases in Tau phosphorylation through a glycogen synthase kinase 3beta-dependent pathway, J. Biol. Chem. 274 (1999) 21395–21401.
[14] A.J. Kim, Y. Shi, R.C. Austin, G.H. Werstuck, Valproate protects cells from ER stress-induced lipid accumulation and apoptosis by inhibiting glycogen synthase kinase-3, J. Cell Sci. 118 (2005) 89–99.
[15] L. Kim, J. Liu, A.R. Kimmel, The novel tyrosine kinase ZAK1 activates GSK3 to direct cell fate specification, Cell 99 (1999) 399–408.
[16] M. Lesort, R.S. Jope, G.V. Johnson, Insulin transiently increases tau phosphorylation: involvement of glycogen synthase kinase-3beta and Fyn tyrosine kinase, J. Neurochem. 72 (1999) 576–584.
[17] S. Liu, S. Yu, Y. Hasegawa, R. Lapushin, H.J. Xu, J.R. Woodgett, G.B. Mills, X. Fang, Glycogen synthase kinase 3beta is a negative regulator of growth factor-induced activation of the c-Jun N-terminal kinase, J. Biol. Chem. 279 (2004) 51075–51081.
[18] S.L. McElroy, P.E. Keck Jr., H.G. Pope Jr., J.I. Hudson, Valproate in psychiatric disorders: literature review and clinical guidelines, J. Clin. Psychiatry. 50 (Suppl.) (1989) 23–29.
[19] M.M. Morgan, E.N. Fossum, C.S. Levine, S.L. Ingram, Antinociceptive tolerance revealed by cumulative intracranial microinjections of morphine into the periaqueductal gray in the rat, Pharmacol. Biochem. Behav. 85 (2006) 214–219.
[20] J.R. Parkitna, I. Obara, A. Wawrzczak-Bargiela, W. Makuch, B. Przewlocka, R. Przewlocki, Effects of glycogen synthase kinase 3beta and cyclin-dependent kinase 5 inhibitors on morphine-induced analgesia and tolerance in rats, J. Pharmacol. Exp. Ther. 319 (2006) 832–839.
[21] J.M. Quillan, K.W. Carlson, C. Song, D. Wang, W. Sadee, Differential effects of mu-opioid receptor ligands on Ca(2+) signaling, J. Pharmacol. Exp. Ther. 302 (2002) 1002–1012.
[22] G. Rosenberg, The mechanisms of action of valproate in neuropsychiatric disorders: can we see the forest for the trees? Cell Mol. Life Sci. 64 (2007) 2090–2103.
[23] W. Solecki, T. Krowka, J. Kubik, L. Kaczmarek, R. Przewlocki, Increased analgesic tolerance to acute morphine in fosB knock-out mice: a gender study, Pharmacol. Biochem. Behav. 90 (2008) 512–516.
[24] A.A. Somogyi, D.T. Barratt, J.K. Coller, Pharmacogenetics of opioids, Clin. Pharmacol. Ther. 81 (2007) 429–444.
[25] C. Sutherland, I.A. Leighton, P. Cohen, Inactivation of glycogen synthase kinase-3 beta by phosphorylation: new kinase connections in insulin and growth-factor signalling, Biochem. J. 296 (Pt 1) (1993) 15–19.
[26] K.A. Trujillo, H. Akil, Inhibition of morphine tolerance and dependence by the NMDA receptor antagonist MK-801, Science 251 (1991) 85–87.
[27] T.L. Yaksh, J.C. Yeung, T.A. Rudy, Systematic examination in the rat of brain sites sensitive to the direct application of morphine: observation of differential effects within the periaqueductal gray, Brain Res. 114 (1976) 83–103.

Anesthesiology 2010; 113:812–8

Sitting Posture Decreases Collapsibility of the Passive Pharynx in Anesthetized Paralyzed Patients with Obstructive Sleep Apnea

Yugo Tagaito, M.D.,* Shiroh Isono, M.D.,† Atsuko Tanaka, M.D.,‡ Teruhiko Ishikawa, M.D.,§ Takashi Nishino, M.D.‖

ABSTRACT

Background: Obstructive sleep apnea (OSA) is an independent risk factor for difficult and/or impossible mask ventilation during anesthesia induction. Postural change from supine to sitting improves nocturnal breathing in patients with OSA. The purpose of this study was to evaluate the effect of patient position on collapsibility of the pharyngeal airway in anesthetized and paralyzed patients with OSA. The authors tested the hypothesis that the passive pharynx is structurally less collapsible during sitting than during supine posture.

Method: Total muscle paralysis was induced with general anesthesia in nine patients with OSA, eliminating neuromuscular factors contributing to pharyngeal patency. The cross-sectional area of the pharynx was measured endoscopically at different static airway pressures. Comparison of static pressure–area plots between the supine and sitting (62° head-up) allowed assessment of the postural differences of the mechanical properties of the pharynx.

Results: Maximum cross-sectional area was greater during sitting than during supine posture at both retropalatal (median (10th–90th percentile): 1.91 (1.52–3.40) *versus* 1.25 (0.65–1.97) cm^2) and retroglossal (2.42 (1.72–3.84) *versus* 1.75 (0.47–2.35) cm^2) airways. Closing pressure of the passive pharynx was significantly lower during sitting than supine posture. Differences of the closing pressures between the postures are 5.89 (3.73–11.6) and 6.74 (4.16–9.87) cm H_2O, at retropalatal and retroglossal airways, respectively, and did not differ between the pharyngeal segments.

Conclusions: Postural change from supine to sitting significantly improves collapsibility of pharyngeal airway in anesthetized and paralyzed patients with OSA.

What We Already Know about This Topic

- Although sitting posture improves symptoms in many patients with obstructive sleep apnea (OSA), whether it alters collapsibility of the pharyngeal airway during anesthesia is unknown

What This Article Tells Us That Is New

- In nine patients with OSA during general anesthesia with neuromuscular blockade, change from supine to sitting position significantly improved collapsibility of the pharyngeal airway

PHARYNGEAL airway obstruction impairs both spontaneous breathing and mechanical ventilation leading to severe hypoxemia during sleep or anesthesia.[1] Presence of obstructive sleep apnea (OSA) is an independent risk factor for difficult and/or impossible mask ventilation during anesthesia induction.[2,3] Establishment of airway management strategies for prevention or reversal of pharyngeal airway obstruction in anesthetized and paralyzed patients with OSA, therefore, is a significant task assigned to anesthesiologists responsible for patients' safety during perioperative periods.

Compared with supine posture, sitting posture is reported to decrease OSA frequency particularly in more obese patients with OSA,[4] suggesting significant improvement of pharyngeal airway patency during sitting posture. However, no study has assessed postural changes of pharyngeal airway dimensions during sleep and anesthesia. In awake patients with OSA, previous studies demonstrated variable influences of sitting posture on the pharyngeal airway dimensions,[5–10] possibly because of compensatory increase of the genioglossal muscle activity in response to the postural change from sitting to supine.[7] Whereas significant decrease of upper airway closing pressure during sitting posture was reported in sleeping patients with OSA,[11] pharyngeal muscle activity was not controlled during the closing pressure measurements in this

* Associate Professor, Department of Anesthesiology, Teikyo University Chiba Medical Center, Ichihara, Japan. † Associate Professor, § Assistant Professor, ‖ Professor, Department of Anesthesiology (B1), Graduate School of Medicine, Chiba University, Chiba, Japan. ‡ Head, Department of Anesthesiology, Seirei Sakura City Hospital, Sakura, Japan.

Received from Department of Anesthesiology (B1), Graduate School of Medicine, Chiba University, Chiba, Japan. Submitted for publication February 2, 2010. Accepted for publication June 29, 2010. Supported by Grant-in-Aid No. 21592000 from the Ministry of Education, Culture, Sports, Science and Technology, Tokyo, Japan.

Address correspondence to Dr. Isono: Department of Anesthesiology (B1), Graduate School of Medicine, Chiba University, 1-8-1 Inohana-cho, Chuo-ku, Chiba, 260-8670, Japan. shirohisono@yahoo.co.jp.

study, and both structural and neural factors contributed to the influences of sitting posture on pharyngeal airway collapsibility.

We have developed a method for exclusively evaluating structural properties of each pharyngeal segment independently of the neural factors[12] and successfully applied the methodology for assessing influences of various mechanical interventions on pharyngeal airway patency under general anesthesia.[13–15] Accordingly, our primary purpose in this study was to test the hypothesis that sitting posture improves pharyngeal airway patency even under absence of neural mechanisms. We compared static pharyngeal mechanics of the passive pharynx during supine posture with those during sitting posture in anesthetized and paralyzed patients with OSA.

Materials and Methods

Subjects and Sleep Studies

Informed consent was obtained from all subjects after the aim and potential risks of the study were fully explained to each. The investigation was approved by the Hospital Ethics Committee (Graduate School of Medicine, Chiba University, Chiba, Japan).

We studied nine consecutive male patients with OSA who were interested in undergoing uvulopalatopharyngoplasty as a treatment for their OSA and were scheduled to have endoscopic assessment of their pharyngeal mechanics to determine whether they were favorable candidates for this procedure.[16] Exclusion criteria in this study included (1) difficulty in performing mandible advancement and head extension, (2) presence of clinical symptoms suggesting chronic heart failure, (3) presence of pulmonary aspiration risk, and (4) presence of a beard, which potentially may cause a mask leak. All had histories of excessive daytime sleepiness, habitual snoring, and witnessed repetitive apnea. Sleep disordered breathing was evaluated by a pulse oximeter (Pulsox-5; Minolta, Tokyo, Japan) at home. All subjects were instructed to attach an oximetry finger probe before sleep and to remove the probe on awakening. After checking quality of the recordings of arterial oxygen saturation (Spo_2), oximetry variables were calculated by computer software.[12–16] Although the oximetry evaluation alone does not clarify the nature of sleep-disordered breathing, we believe that all nine patients can be safely diagnosed as having OSA based on the oximetry results and the clinical symptoms.[17] OSA diagnosis was confirmed by standard full polysomonography in seven patients with OSA. Recordings include bilateral electroencephalograms, bilateral electrooculograms, submental electromyogram, leg electromyograms, electrocardiogram, airflow measurement with a thermistor at the mouth and nose, thoracoabdominal wall motions, Spo_2, snoring over a microphone, and body position. Apnea was defined as absence of airflow for more than 10 s. Hypopnea was determined upon an apparent reduction of airflow for more than 10 s with reduction of Spo_2 by more than 4% from the baseline. Apneic events were classified as obstructive, mixed, and central, and the apnea-hypopnea index was calculated as the total number of the obstructive or mixed apnea and hypopnea events per hour of sleep.

Preparation of the Subjects

Each subject was initially premedicated with 0.5 mg atropine. Studies were performed with the subjects in either supine position or sitting at a 62° angle on an adjustable medical stretcher trolley, with the neck in a comfortable neutral position. The sitting angle was chosen because it was the most upright position safe for an anesthetized and paralyzed patient without restraint equipment. A modified tight-fitting nasal mask was used. Care was taken to prevent air leaks from the mask, particularly when the airway was pressurized above 20 cm H_2O. Use of a chin strap maintained contact of the upper and lower incisors and eliminated air leaks through the mouth. Air leaks through the mask and mouth were detected by inadequate increase in the airway pressure (P_{AW}) and manual palpation. General anesthesia was induced by intravenous infusion of propofol (2 mg/kg) and intravenous injection of a muscle relaxant (vecuronium 0.2 mg/kg). General anesthesia with total paralysis was maintained by continuous infusion of propofol (6–10 mg · kg^{-1} · h^{-1}) while the subject was ventilated through the nasal mask with positive pressure through an anesthetic machine. Complete paralysis was confirmed by no responses to train-of-four stimulations at the ulnar nerve. Spo_2 and an electrocardiogram were continuously monitored, and blood pressure was noninvasively measured every 5 min. A slim endoscope (3 mm OD; FB10×; Pentax, Tokyo, Japan) was inserted through a 10-mm diameter hole in a modified nasal mask and into a naris (fig. 1). A modified silicone rubber plug with continuous bubbles (15 mm OD; SILICOSEN type L; Shin-Etsu Polymer Co., Ltd., Tokyo, Japan) tightly plugged the hole and held the endoscope to prevent leakage around them. The tip of the scope was placed at the upper airway to visualize the retropalatal airway space (airway space behind the soft palate) and the retroglossal airway space (airway space behind the base of the tongue). A closed-circuit camera (ETV8; Nisco, Saitama, Japan) was connected to the endoscope, and the pharyngeal images were recorded on a video-

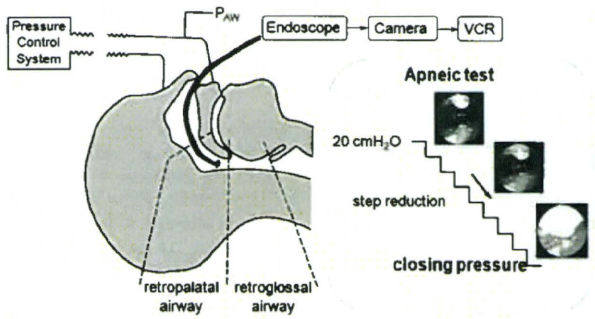

Fig. 1. Experimental setting. The detailed explanation is under Materials and Methods (Preparation of the Subjects). P_{AW} = airway pressure.